A co-opted endogenous retroviral envelope promotes cell survival by controlling CTR1-mediated copper transport and homeostasis

Sandrine Tury, Lise Chauveau, Arnaud Lecante, Valérie Courgnaud, Jean-Luc Battini

Cell Reports

Article

A co-opted endogenous retroviral envelope promotes cell survival by controlling CTR1-mediated copper transport and homeostasis

Graphical abstract

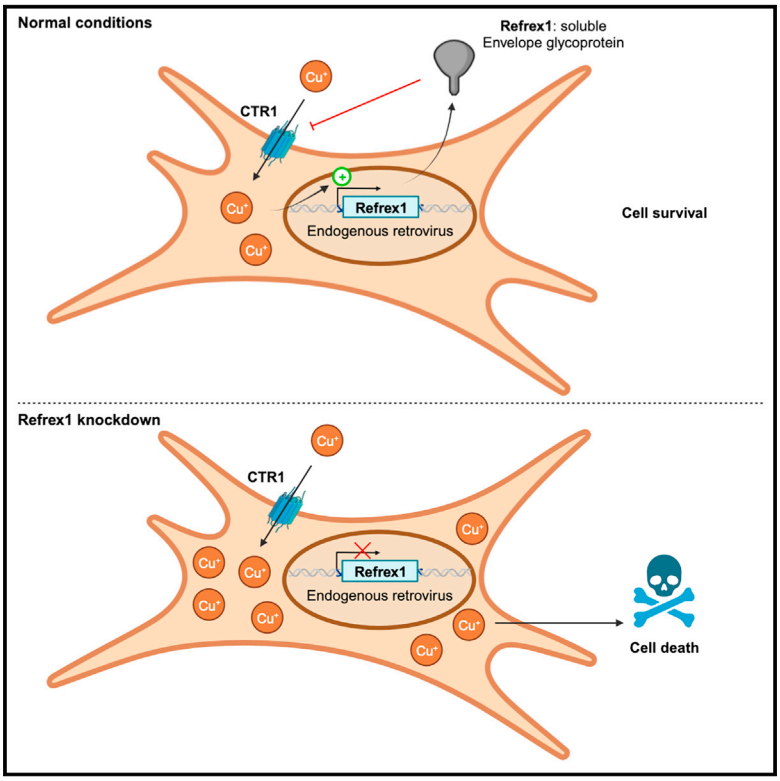

Highlights

- Copper transporter CTR1 is the sole receptor for the endogenous retroviral Env Refrex1
- Refrex1 controls CTR1-dependent copper accumulation
- Cat cells respond to elevated copper by increasing Refrex1 expression
- Refrex1 silencing induces cell death by apoptosis in a copper-dependent manner

Authors

Sandrine Tury, Lise Chauveau, Arnaud Lecante, Valérie Courgnaud, Jean-Luc Battini

Correspondence

valerie.courgnaud@igmm.cnrs.fr (V.C.), jean-luc.battini@irim.cnrs.fr (J.-L.B.)

In brief

Tury et al. show that evolutionary co-option of the ERV envelope glycoprotein Refrex1 in domestic cats represents a mechanism for copper homeostasis. Under elevated copper conditions, Refrex1 is upregulated and interacts with CTR1 to downmodulate copper transport. Cells deficient in Refrex1 accumulate intracellular copper, leading to cell death by apoptosis.

Tury et al., 2023, Cell Reports *42*, 113065
September 26, 2023
https://doi.org/10.1016/j.celrep.2023.113065

CellPress

Cell Reports

CellPress
OPEN ACCESS

Article

A co-opted endogenous retroviral envelope promotes cell survival by controlling CTR1-mediated copper transport and homeostasis

Sandrine Tury,[1,3] Lise Chauveau,[1,3] Arnaud Lecante,[1] Valérie Courgnaud,[2,*] and Jean-Luc Battini[1,4,*]
[1]Institut de Recherche en Infectiologie de Montpellier IRIM – CNRS UMR 9004, Université Montpellier, 34293 Montpellier Cedex 5, France
[2]Institut de Génétique Moléculaire de Montpellier IGMM – CNRS UMR 5535, Université Montpellier, 34293 Montpellier Cedex 5, France
[3]These authors contributed equally
[4]Lead contact
*Correspondence: valerie.courgnaud@igmm.cnrs.fr (V.C.), jean-luc.battini@irim.cnrs.fr (J.-L.B.)
https://doi.org/10.1016/j.celrep.2023.113065

SUMMARY

Copper is a critical element for eukaryotic life involved in numerous cellular functions, including redox balance, but is toxic in excess. Therefore, tight regulation of copper acquisition and homeostasis is essential for cell physiology and survival. Here, we identify a different regulatory mechanism for cellular copper homeostasis that requires the presence of an endogenous retroviral envelope glycoprotein called Refrex1. We show that cells respond to elevated extracellular copper by increasing the expression of Refrex1, which regulates copper acquisition through interaction with the main copper transporter CTR1. Downmodulation of Refrex1 results in intracellular copper accumulation leading to reactive oxygen species (ROS) production and subsequent apoptosis, which is prevented by copper chelator treatment. Our results show that Refrex1 has been co-opted for its ability to regulate copper entry through CTR1 in order to limit copper excess, redox imbalance, and ensuing cell death, strongly suggesting that other endogenous retroviruses may have similar metabolic functions among vertebrates.

INTRODUCTION

Copper is an essential element for the development of all forms of eukaryotes. Copper ions exist in two redox states, the cuprous ion Cu^{+} and the cupric ion Cu^{2+}. This Cu^{+}/Cu^{2+} redox couple is a powerful cargo of electrons and is therefore critical for a multitude of enzymatic reactions that are essential for cellular functions, including cellular respiration and free radical detoxification.[1,2] However, copper excess is toxic, as it affects the cellular redox balance leading to unwanted toxic reactive oxygen species (ROS). Therefore, copper homeostasis is tightly controlled to meet both copper sufficiency and toxic limitation. It relies on regulated mechanisms involving multiple cellular factors with key roles in copper acquisition, in sequestering and chaperoning copper for proper distribution, and in excretion. Copper transporters are particularly important in this process, with the ATPase pumps ATP7A and ATP7B concentrating copper into the *trans*-Golgi network and the main plasma membrane-localized copper transporter 1 SLC31A1/CTR1 importing Cu^{+} from the extracellular environment.[2] In the situation of copper excess in human cells, ATP7A and ATP7B relocate to the plasma membrane and release copper, while CTR1 is endocytosed to prevent excessive copper uptake.[3] Other cellular adaptations include the cleavage of the CTR1 ectodomain by cathepsins in a CTR2-dependent manner leading to reduced copper binding to CTR1 and subsequent uptake.[4–6] Such specialized mechanisms have been adopted by organisms during evolution, which suggests that other important regulators of the copper homeostasis machinery may exist in vertebrates.

Retrovirus-vertebrate interaction is a recognized factor of evolution that has shaped genomes with hundreds of inherited retroviral sequences.[7] In humans, 42% of genomic DNA sequences have retroviral origins, of which 8% are endogenous retroviruses (ERVs) with a genetic organization similar to that of modern exogenous retroviruses.[8,9] Although most ERVs are inactive due to accumulation of deleterious mutations,[9] rare ERV genes have been co-opted by hosts for cellular functions. To date, the co-option of more than 80 retroviral *env* genes has been identified in vertebrates,[10] including 18 in humans.[11,12] These *env* genes encode envelope glycoproteins (Envs) with receptor recognition, membrane fusion, and immunosuppressive properties.[13] Co-opted Envs retaining receptor-binding properties have often been described as restriction factors in various animals for their capacity to confer resistance to exogenous infections via receptor saturation,[14–18] but several of them have been reassigned by hosts for physiological functions. These include the human ERV HERV-W and HERV-FRD Envs, renamed syncytins for their role in syncytiotrophoblast formation during placentation,[19,20] as well as non-human syncytins found in numerous mammals.[13] Another co-opted Env originating from HERV-K subtype HML2 is involved in stemness maintenance to avoid neuronal differentiation through the regulation of the mTOR

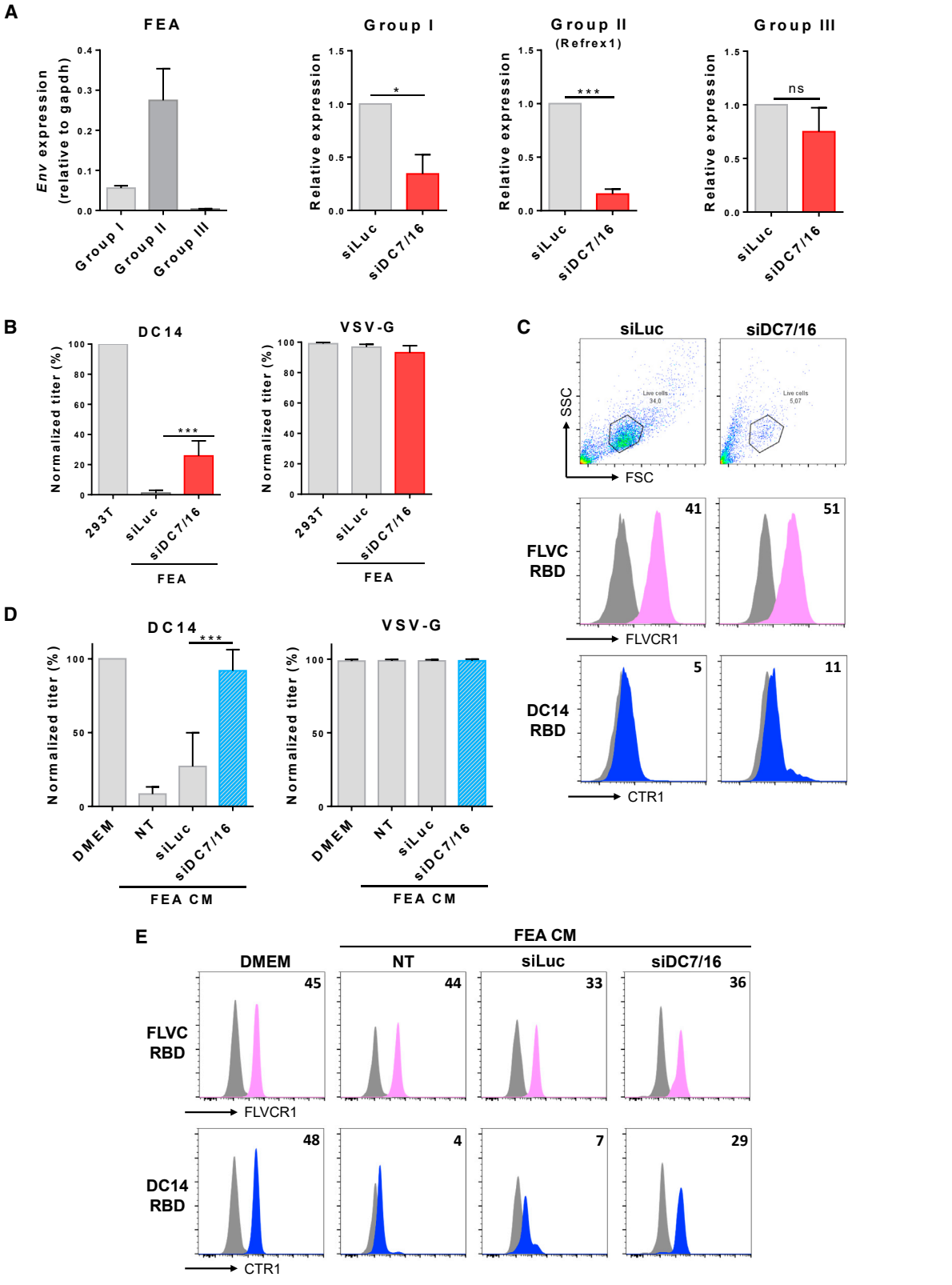

(legend on next page)

pathway.[21] Most ERVs originated from ancient gammaretroviruses, and all their retroviral receptors identified so far are members of a large family of cell-surface nutrient transporters (solute carriers; SLCs) involved in cell metabolism[22]; thus, their interaction with retroviral Envs often affects nutrient transport.[23–26] Therefore, in addition to their roles as restriction factors, as regulators of stemness, or as fusogenic molecules for placentation, it is not excluded that endogenous Envs could act as modulators of cellular metabolism.

In domestic cats, two endogenous categories of ERVs express a truncated receptor-binding domain (RBD) Env, namely FeLIX and Refrex1.[16,27] FeLIX is related to the feline leukemia virus type B (FeLV-B) endogenous Env[28] and, as such, is able to bind the SLC20A1/PiT1 phosphate transporter.[29] On the other hand, Refrex1 is related to the ERV-DC domestic cat ERV family,[30] is expressed from the ERV-DC7 and ERV-DC16 loci, and has been described as a restriction factor against ERV-DC infection.[16,31] ERV-DC7 and -DC16 loci are fixed in domestic cats as well as in European wild cats (ERV-DC7 only) and are actively transcribed, suggesting that Refrex1 activity has been evolutionarily conserved in cats.[31–33] We and others have recently shown that the copper transporter CTR1 is a retroviral receptor for FeLV-D/Refrex1-related ERV-DC.[34,35] In this study, we asked whether Refrex1, in addition to its role as a restriction factor, has been co-opted for a more physiological function. We report that Refrex1 is involved in cell survival by controlling copper homeostasis via its receptor CTR1 and that Refrex1 expression is itself regulated by extracellular copper, suggesting the presence of a copper-sensing feedback loop in which Refrex1 plays a central role. Thus, co-option of endogenous *env* genes by the host could also be envisioned as a selective advantage for proper cell metabolism and survival.

RESULTS

ERV-DC7/16 *env* gene silencing restores ERV-DC14 binding and infection in feline FEA cells

Refrex1 was first described as a soluble antiretroviral factor present in wild and domestic cats and in the culture medium of several cat cell lines,[16] but it is not known whether Refrex1 also plays a physiological role in these cells. We first evaluated by qRT-PCR the expression level of the three genotype groups of ERV-DC *env* transcripts in feline FEA cells, namely, group I (ERV-DC2, 8, 14, 17, and 19); group II (ERV-DC7 and 16), encoding Refrex1; and group III (ERV-DC6, 10, and 18). We found that group II mRNAs were highly expressed in FEA cells, in much higher amounts than those of genotype groups I and III (Figure 1A, left), suggesting a predominance of Refrex1 expression over the other ERV-DC Envs. Surprisingly, we detected only the expression of the ERV-DC16 mRNA in FEA cells, and the same observation was made in feline CRFK cells, suggesting that the ERV-DC7 locus was inactive in these two feline cell lines (Figure S1A). Nevertheless, both ERV-DC7 and ERV-DC16 mRNAs were expressed in primary cat peripheral blood mononuclear cells (PBMCs) (Figure S1A). We next designed an siRNA (siDC7/16) targeting a common sequence in ERV-DC7 and ERV-DC16 *env* genes to silence Refrex1 expression (Figure S1B). Transfection of FEA cells by siDC7/16, but not by an siRNA control targeting the firefly *luciferase* gene (siLuc), decreased the level of group II mRNAs significantly and, to a lesser extent, those of group I, despite two mismatches within the siDC7/16 sequence (Figure 1A, right). All feline cell lines are resistant to ERV-DC14 pseudotype infection, including FEA cells (Figure 1B). We observed that Refrex1 silencing increased by 20-fold the infectivity of lentiviral vector particles carrying the *GFP* gene pseudotyped with the ERV-DC14 Env (Figure 1B) and increased the binding of an ERV-DC14 immunoadhesin comprising an Env RBD fused to a mouse IgG1 Fc fragment (DC14RBD) (Figures 1C and S1C). We recently showed that the retroviral receptor recognized by this DC14RBD immunoadhesin is the copper transporter CTR1.[34] In contrast, binding of the FeLV-C Env RBD (FLVCRBD), which recognizes the heme transporter FLVCR1, was unchanged. Thus, the presence of Refrex1 in FEA cells is responsible for the resistance to ERV-DC14 pseudotype infection, presumably by saturating CTR1.[34,35] We also tested the presence of Refrex1 in FEA-conditioned medium (CM) by measuring its inhibitory activity on ERV-DC14 infectivity and binding. Pretreatment of human 293T cells with FEA-CM demonstrated a strong decrease in both ERV-DC14 pseudotype infection, as expected,[16] and DC14RBD binding, while infectivity of vesicular stomatitis virus G protein (VSV-G)-pseudotyped particles was unchanged, as well as FLVCRBD binding (Figures 1D and 1E). In contrast, CM of siDC7/16-transfected FEA cells was unable to inhibit Env binding and infection with ERV-DC14 (Figures 1D and 1E), suggesting that the release of Refrex1 in FEA CM was abolished. This also demonstrated that Refrex1 was expressed solely from ERV-DC7 and 16 loci. Unexpectedly, we found that Refrex1 silencing was accompanied by cell toxicity, as observed by the low percentage of gated cells in the siDC7/16 dot plot of Figure 1C.

Figure 1. Refrex1 is the only factor controlling the retroviral receptor function of CTR1 in feline cells

(A) ERV-DC *env* gene expression from genotype groups I, II, and III was evaluated by qRT-PCR of cells and normalized with cat Gapdh in non-transfected FEA cells (left) or after transfection with siDC7/16 targeting both ERV-DC7 and DC16 *env* or with an siRNA control (siLuc) (three right bar plots). Fold changes are normalized to siLuc. Data are means ± SEM from n = 3 independent experiments. Student's unpaired t test, $^{*}p \leq 0.05$, $^{***}p \leq 0.001$.

(B) Sensitivity of siDC7/16- or siLuc-transfected FEA cells to infection by EGFP lentiviral vectors pseudotyped with ERV-DC14 or VSV-G Env. 293T target cells were used as control and for normalization. Data are means ± SEM from n = 3 independent experiments. Student's unpaired t test, $^{***}p \leq 0.001$.

(C) Cells from (B) were evaluated for FLVC and DC14 Env RBD binding by flow cytometry. Forward-scatter (FSC) versus side-scatter (SSC) plots show gated living cells. Numbers indicate the specific change in mean fluorescence intensity compared with non-specific mock staining (gray histogram). Representative experiment of n = 3 biological replicates.

(D) 293T cells incubated in conditioned medium (CM) from feline FEA cells transfected or not with the indicated siRNA or in DMEM for 5 h were evaluated for their sensitivity to infection by EGFP lentiviral vectors pseudotyped with VSV-G or ERV-DC14 Env. NT, non-transfected. Data are means ± SEM from n = 3 independent experiments. Student's unpaired t test, $^{***}p \leq 0.001$.

(E) Cells from (D) were evaluated for RBD binding as in (C). Representative experiment from n = 3 biological replicates.

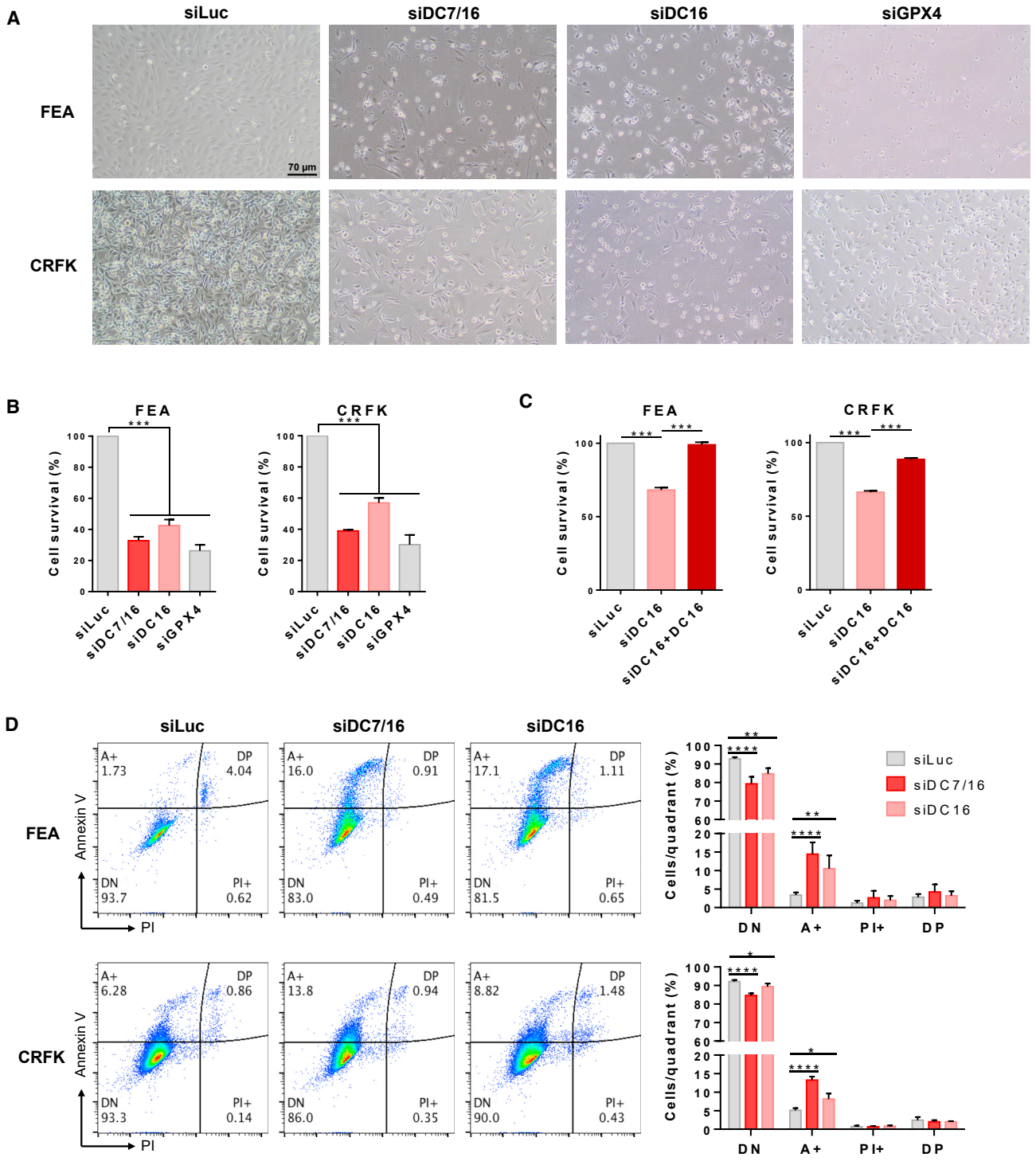

Figure 2. Inactivation of Refrex1 expression induces cell death

(A) Representative images of feline FEA and CRFK cells transfected with siDC7/16, siDC16, siLuc control, or an siRNA targeting feline GPX4 mRNA (siGPX4) under bright light using a Nikon Eclipse Ts2 microscope. Scale bar, 70 µm.

(B) Cellular viability of cells from (A) was evaluated 48 h post-transfection using CellTiter 96 AQueous One Solution cell proliferation assay. Data are means ± SEM from n = 3 independent experiments. One-way ANOVA with Dunnett's multiple comparisons test, ***p ≤ 0.001.

(legend continued on next page)

Loss of Refrex1 expression induces cell death by apoptosis

The concomitant loss of Refrex1 and appearance of cell toxicity upon siDC7/16 transfection may suggest a role for Refrex1 in cell survival. Transfection of FEA cells by two different siRNAs able to silence Refrex1, siDC7/16 and siDC16, targeting only the DC16 *env* gene (Figure S1B), confirmed the observed toxic effect as seen by phase-contrast microscopy and by enzymatic assay (Figures 2A and 2B) at levels similar to those of glutathione peroxidase 4 (GPX4) silencing known to induce ferroptosis.[36] Toxicity was not specific to FEA cells, since we observed the same effect in CRFK cells, albeit less pronounced, and this in a dose-dependent manner (Figures 2A, 2B, and S2A). Moreover, toxicity was readily observed 24 h after transfection in FEA cells, but took longer in CRFK cells, suggesting that both cell lines have different sensitivities toward Refrex1 depletion (Figure S2B). In contrast, this defect was observed neither with the siLuc control nor with siDC7/16- or siDC16-transfected human cells that do not express Refrex1 (Figure S2C). To assess whether this was due to an indirect effect or was attributed specifically to loss of DC16 Env, we performed a rescue experiment assay using a DC16 *env* expression vector. As expected, transfection of FEA and CRFK cell lines with siDC16 affected cell survival even in combination with an empty expression vector (Figure 2C). In contrast, cell survival was fully restored after reexpression of DC16 Env (Figure 2C) from an expression vector insensitive to siDC16 (Figure S1B). We next asked what type of cell death was responsible for the observed cell toxicity. Compared with mock-transfected FEA and CRFK cells, Refrex1 silencing increased the percentage of Annexin V-positive cells by 4-fold at 24 h post-transfection, a time point before excessive cell death (Figure 2D). As mentioned above, the cell death was delayed in CRFK cells, and they showed a lower proportion of Annexin V-positive cells at 24 h (Figure 2D). Thus, these results point to Refrex1 as an essential factor protecting feline cells from apoptosis.

CTR1 is a potent and the sole receptor for Refrex1

Since Refrex1 is an Env ligand able to interfere with ERV-DC14 infection by receptor saturation,[16,35] we reasoned that its receptor-binding property would be critical to prevent cell death. We and others have recently identified the copper transporter CTR1 (Figure 3A) as a retroviral receptor for ERV-DC14 and FeLV-D as well as for Refrex1.[34,35] However, it is not excluded that Refrex1 can recognize additional receptors at the plasma membrane. To answer this question, we employed a flow cytometry assay with a Refrex1 ligand derived from ERV-DC16 *env* and harboring three copies of the hemagglutinin (HA) tag in place of the natural stop codon (DC16RBD). DC16RBD elicited strong binding on human 293T cells, but no binding was observed on hamster CHO cells known to be resistant to ERV-DC14 infection (Figures 3C and 3E). Introduction of human or feline *CTR1* cDNA into hamster CHO cells (Figure 3B) conferred strong binding to RBD but did not alter the binding of the FLVCRBD (Figure 3C). Therefore, our results confirmed that CTR1 is a potent and specific receptor for Refrex1, consistent with the antiviral property of Refrex1.[34,35] We next asked whether CTR1 was the only cell-surface receptor for Refrex1. Inactivation of the *CTR1* gene in 293T cells by genome editing fully abolished the global expression of CTR1 (Figure 3D) as well as its specific presence at the plasma membrane using an anti-human CTR1 antibody (Figure 3E). Depletion of CTR1 led to a dramatic loss of DC16RBD binding, while FLVCRBD binding remained unchanged (Figure 3E). Another means of downmodulating CTR1 expression from the surface of human cells is exposure to a high dose of copper.[3,34,37] Figure 3F indicates that overnight treatment of human 293T cells with 100 μM copper chloride specifically decreased DC16RBD binding, while magnesium chloride had no effect. Overall, these data indicate that CTR1 is a specific and the sole receptor for Refrex1.

Refrex1 regulates copper transport and homeostasis

Interaction between retroviral Envs and their cognate receptors often leads to decreased transporter activities.[23–26] Since Refrex1 is derived from retroviral Env sequences, we tested whether it could alter copper transport. We first expressed Refrex1 in 293T cells from *ERV-DC7* and *16 env* expression vectors either alone or in combination. Both vectors expressed C-terminal HA-tagged *ERV-DC7* and *16 env* gene products. We confirmed that both Refrex1 isoforms were properly expressed and secreted in the culture medium of transfected human 293T cells (Figure 4A) and that their presence alone or in combination conferred a strong resistance to infection by ERV-DC14 pseudotypes (Figure 4B) and abolished the binding of DC14RBD (Figure 4C). We then measured the intracellular content of free copper in 293T cells by mass spectrometry. We found that copper levels were slightly but significantly reduced in the three conditions compared with control, while levels of magnesium were unchanged (Figure 4D). We then performed the reverse experiment in feline cells, in which Refrex1 was silenced by transfection of siDC16. As expected, a specific increase in copper level was observed in the absence of Refrex1 in both FEA and CRFK cells (Figure 4E), suggesting that Refrex1 can control copper homeostasis by modulating copper transport through CTR1. This modulation was not due to CTR1 degradation nor to its cell-surface downmodulation by Refrex1 as observed using human and feline CTR1 constructs harboring an N-terminal FLAG tag exposed to the extracellular environment (Figures S3A–S3F). We reasoned that changes in intracellular copper level would affect the expression of genes encoding actors in copper homeostasis, like transporters and metallothionein (MT1/2) storage proteins. Although we found non-significant increase in *ATP7A* and *ATP7B* gene expression, both encoding copper exporters, as well as *COMMD1*, also assisting copper export, we observed a

(C) FEA and CRFK cells were transfected with siLuc or siDC16 in combination with an empty vector or with DC16 Env expression vector. Cell viability was evaluated as in (B). Data are means ± SEM from n = 3 independent experiments. One-way ANOVA with Dunnett's multiple comparisons test, ***$p \leq 0.001$.
(D) FEA and CRFK cells transfected with siLuc, siDC7/16, or siDC16 were stained with Annexin V/propidium iodide (PI) at 24 h post-transfection. Pseudocolor plots from a representative experiment (left) and means ± SEM from at least n = 3 independent experiments (right histograms) are shown. DN, double-negative cells; A+, Annexin V-positive cells; DP, double-positive cells. Two-way ANOVA with Sidak's multiple comparisons test, *$p \leq 0.05$, **$p \leq 0.01$, ****$p \leq 0.0001$.

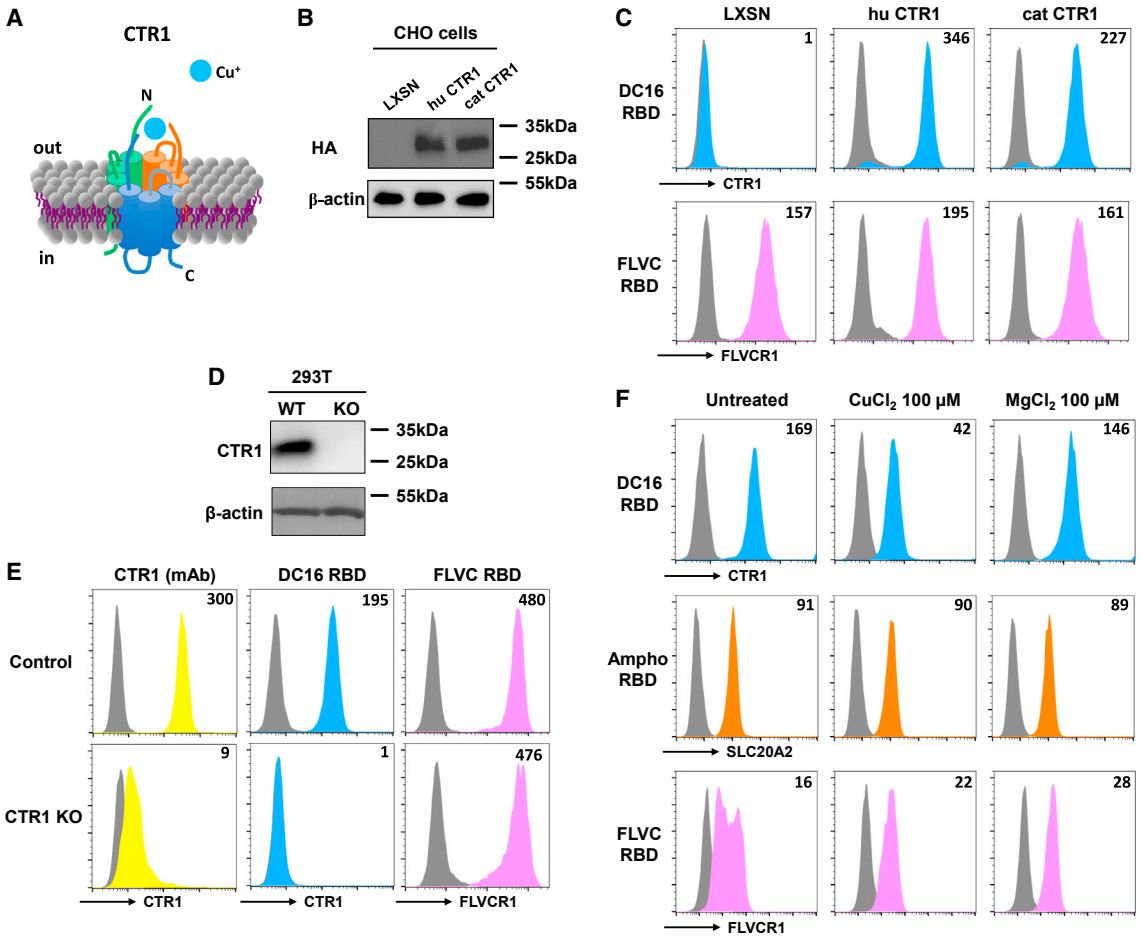

Figure 3. Refrex1 interacts with CTR1

(A) Graphical representation of the CTR1 copper transporter.

(B) Representative immunoblot of HA-tagged CTR1 in lysates from Chinese hamster ovary (CHO) cells stably transduced with murine leukemia virus (MLV)-based LXSN retroviral vector[38] either empty or carrying the human (hu) or cat *CTR1* cDNA.

(C) CHO cells from (B) were evaluated for DC16RBD and FLVCRBD binding by flow cytometry. Numbers indicate the specific change in mean fluorescence intensity compared with non-specific mock staining (gray histogram) of a representative experiment (n = 3 biological replicates).

(D) Detection of CTR1 by immunoblot in cell lysates of 293T cells either parental (WT) or KO for CTR1 (CTR1 KO) as generated by CRISPR-Cas9 technology.

(E) Cells from (D) were evaluated as in (C) using the indicated RBD ligands or an anti-CTR1 mAb. Representative experiment (n = 3 biological replicates). Numbers indicate the specific change in mean fluorescence intensity compared with non-specific mock staining (gray histogram) of a representative experiment (n = 3 biological replicates).

(F) 293T cells grown in 100 μM $CuCl_2$ or $MgCl_2$ overnight were evaluated for CTR1 (DC16RBD), SLC20A2 (AmphoRBD), and FLVCR1 (FLVCRBD) cell-surface expression by flow cytometry using the indicated RBD ligands. Numbers indicate the specific change in mean fluorescence intensity compared with non-specific mock staining (gray histogram) of a representative experiment (n = 3 biological replicates).

strong increase in *MT1/2* mRNA expression (Figure 4F). Surprisingly, *CTR1* expression was not reduced upon Refrex1 depletion and copper accumulation, suggesting that feline cells were unable to regulate copper entry via the control of *CTR1* transcription. Moreover, we found that copper chaperone for SOD1 (CCS) was decreased upon siDC16 expression, which is expected when copper accumulates intracellularly (Figure 4G).[39,40] Cellular copper is known to modulate oxidative phosphorylation (OXPHOS) activities and ROS production.[41] Consistent with this, we found that Refrex1 silencing increased the level of ROS (Figure 4H), while ATP levels were barely affected (Figure 4I). Overall, these results suggest that Refrex1 silencing leads to copper accumulation and subsequent reprogramming of genes involved in copper homeostasis and ROS production independent of ATP synthesis.

Refrex1 expression is modulated by extracellular copper

Human cells can adapt to elevated copper concentration by reducing the level of CTR1 at the plasma membrane, as seen in Figure 3F and as reported.[3] It is not known whether feline cells can sense and respond to extracellular copper in a similar manner. We attempted to detect CTR1 at the plasma membrane of feline cells, but neither our Env ligand DC14RBD nor an

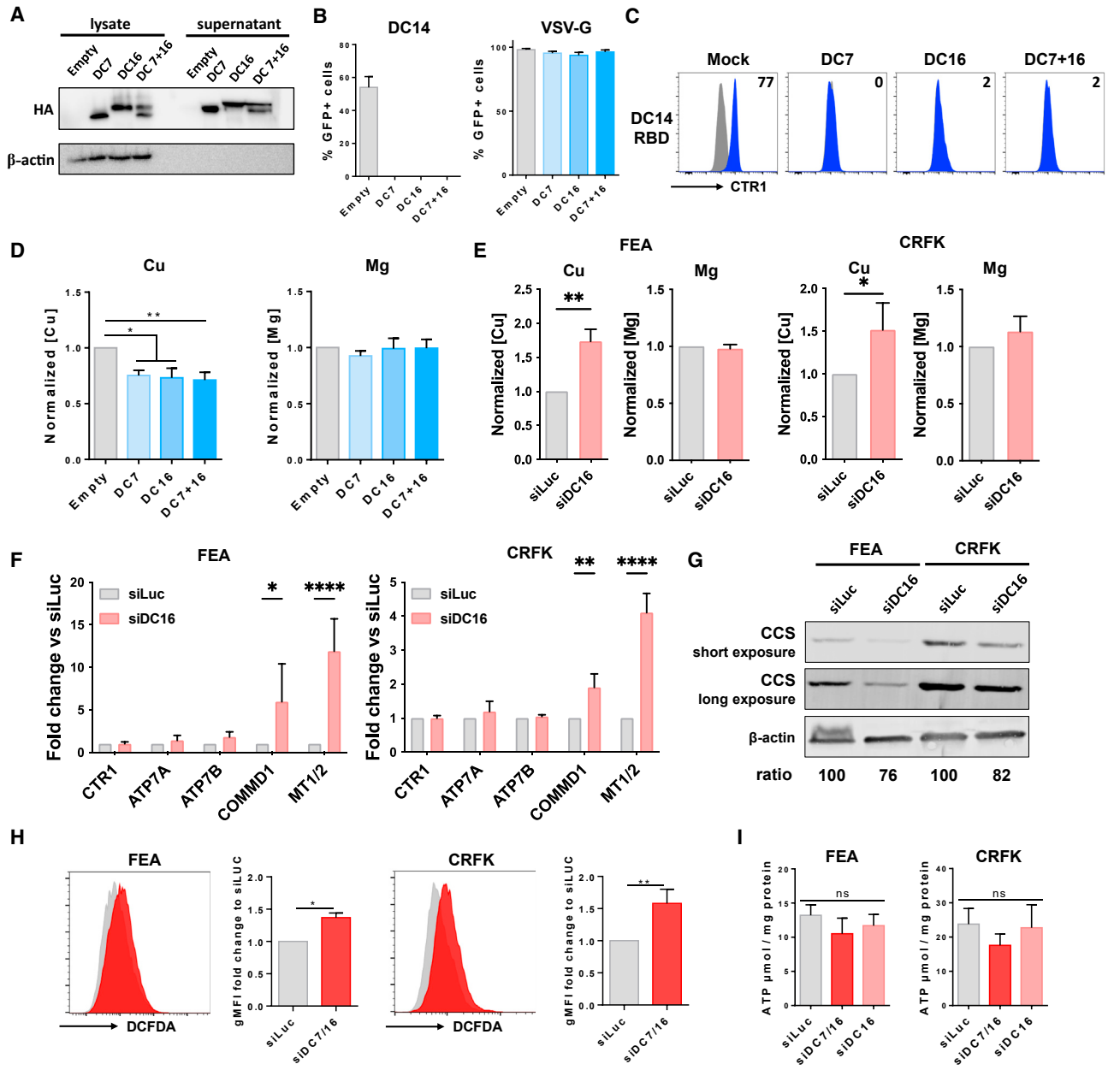

Figure 4. Altered copper homeostasis in the absence of Refrex1 in cat cells

(A) Detection of HA-tagged Refrex1 by immunoblot in cell lysates and supernatants of 293T cells overexpressing empty vector pCHIX or DC7 or DC16 alone or in combination (DC7 + DC16).

(B) Sensitivity of cells from (A) to infection by EGFP lentiviral vectors pseudotyped with ERV-DC14 or VSV-G Env. Data are means ± SEM from n = 3 independent experiments.

(C) Cells from (A) were evaluated for DC14RBD binding by flow cytometry. Numbers indicate the specific change in mean fluorescence intensity compared with non-specific mock staining (gray histogram) of a representative experiment (n = 3 biological replicates).

(D) Total amount of copper (Cu) or magnesium (Mg) was evaluated 48 h post-transfection by inductively coupled plasma mass spectrometry (ICP-MS) in 293T cells from (A). Data are means ± SEM from n = 3 independent experiments. One-way ANOVA with Dunnett's multiple comparisons test, *p ≤ 0.05, **p ≤ 0.01.

(E) Total amount of copper (Cu) or magnesium (Mg) was evaluated by ICP-MS 48 h after transfecting feline FEA and CRFK cells with siLuc or siDC16 (n = 3). Data are means ± SEM from n = 3 independent experiments. Mann-Whitney test, *p ≤ 0.05, **p ≤ 0.01.

(F) mRNA expression of several genes involved in copper homeostasis (*CTR1*, *ATP7A*, *ATP7B*, *COMMD1*, and *MT1/2*) was evaluated by qRT-PCR in feline FEA and CRFK cells transfected with siDC16 or control siLuc and normalized to cat *GAPDH*. Graphs represent the ratio of normalized expression of indicated genes in siDC16-transfected cells to normalized expression in siLuc-transfected cells. Data are means ± SEM from at least n = 3 independent experiments. Two-way ANOVA with Sidak's multiple comparisons test, *p ≤ 0.05, **p ≤ 0.01, ****p ≤ 0.0001.

(legend continued on next page)

antihuman CTR1 antibody was able to recognize the feline CTR1 by flow cytometry (Figures S4A and S4B), due to the capacity of Refrex1 to saturate CTR1. In contrast, CTR1 was reproducibly detected by flow cytometry using a chimpanzee ERV type 2 (CERV2) RBD ligand (Figure S4B).[37] We therefore evaluated CTR1 cell-surface expression after exposure of FEA, CRFK, and human cells to 100 μM copper, as well as zinc and magnesium as metal controls. As expected, we found that CTR1 was downmodulated in human 293T cells in the presence of elevated copper, but, surprisingly enough, CTR1 expression on feline cells remained unchanged in the same conditions (Figure 5A). This was not an intrinsic property of feline CTR1, as its expression as an N-terminal FLAG-tag protein on the surface of 293T CTR1 KO cells was modulated by elevated copper (Figures S4C and S4D). CTR1 expression remained unchanged at the transcriptional level (Figure 5B). Since feline cells have selected Refrex1 as a CTR1 co-factor and as a modulator of copper entry into cells, we next tested the possibility that feline cells would respond to an excess of extracellular copper by modulating Refrex1 expression. To test this hypothesis, FEA and CRFK cells were incubated with increasing amounts of copper, and *ERV-DC7/16* mRNA expression was assessed 24 h later by semi-quantitative RT-PCR. We found that Refrex1 mRNAs were upregulated by elevated extracellular copper levels in a dose-dependent manner (Figures 5C and 5D). This upregulation was specific to copper, since no change in *Refrex1* mRNA expression was observed in the presence of zinc or magnesium (Figure 5E). Overall, these results suggest that adaptation of feline cells to copper excess does not involve CTR1 endocytosis as seen in human cells, but rather they increase expression of Refrex1 to downmodulate copper acquisition through CTR1.

Copper chelator BCS rescues Refrex1-silenced cells from death

The cell death observed in Refrex1-silenced feline cells correlates with the induction of ROS production and subsequent apoptosis, but the exact role of Refrex1 in this process is not known. Since Refrex1 can modulate copper entry via CTR1 interaction, we directly investigated the role of copper in cell death. FEA and CRFK cells transfected with siDC7/16 or control siLuc were grown for 72 h in medium containing the copper chelator bathocuproinedisulfonic acid (BCS), and then cell survival was measured. We found that the induced cell death following Refrex1 silencing was reduced when extracellular copper was neutralized by BCS, as observed by phase-contrast microscopy and crystal violet dosage for FEA cells and to some extent for CRFK cells (Figures 6A and 6B). FEA cell rescue was dose dependent, since the percentage of cell survival gradually reached 100% of siLuc-transfected cells with increasing amounts of BCS. We next assessed the direct impact of copper chelation via BCS treatment on the induction of apoptosis following siDC7/16 transfection. At 24 h, BCS decreased the proportion of Annexin V-positive cells in FEA and, to a lesser extent, in CRFK cells (Figure 6C). Overall, these results suggest that, upon Refrex1 silencing by siRNA, an excess of copper could lead to an apoptotic cell death and that sensitivity to this copper-induced death is cell-type dependent.

Refrex1 is present in cat serum and is induced by copper in primary cells

The presence of Refrex1 has been observed in the culture medium of all feline cell lines tested so far,[16] including in FEA and CRFK-CM (Figures 1D and S5). In contrast, Refrex1 is not expressed in all feline tissues; however, the expression of *ERV-DC7* and *16* mRNA in PBMCs and other tissues may suggest that Refrex1 is present in cat serum.[16] To test this hypothesis, we measured the inhibitory activity of cat sera toward ERV-DC14 infection and DC14RBD binding. We found that cat serum strongly interfered with ERV-DC14 pseudotype infection and Env binding (Figures 7A and 7B) when 293T cells were preincubated with Dulbecco's modified Eagle's medium (DMEM) supplemented with cat serum. Serial dilutions of serum further revealed a 50% decrease in infection after a 500-fold dilution and a total loss of inhibition at a dilution threshold of 1,000-fold, suggesting the presence of Refrex1 at high levels in this circulating body fluid. Consistent with this finding, DC14RBD was unable to bind to freshly isolated cat red blood cells, likely due to interference from serum Refrex1 (Figure 7C). Finally, we tested whether the copper dependence of Refrex1 expression found in FEA and CRFK cells was also observed in cat PBMCs. PBMCs were isolated from the blood of three domestic cat donors and incubated in the presence of copper for 24 h. In the absence of copper, we found a high variability in Refrex1 expression from one donor to another, and this expression was increased in the presence of copper in the PBMCs of two of three cats (Figure 7D). This result suggests that copper sensing exists *in vivo* and that PBMCs may have the capacity to adapt their Refrex1 expression in response to copper variation in cat blood.

DISCUSSION

In this study, we describe a mechanism for copper homeostasis involving the regulation of CTR1-mediated copper acquisition by a co-opted retroviral Env, and we provide evidence that co-option of Refrex1, the Env product expressed from the ERV-DC7 and ERV-DC16 loci of modern cats, is crucial for cell survival. Refrex1 has maintained receptor-binding capacity during cat evolution and inhibitory properties against retroviral receptor function, explaining why Refrex1 was first identified as a restriction factor of exogenous infection.[16,32,33] Here, we further show that Refrex1 affected CTR1-mediated copper transport within cells and subsequent homeostasis, as demonstrated by the

(G) Detection of CCS by immunoblot in cell lysates of FEA and CRFK cells transfected either with siLuc or with siDC16. Exposure at two different times for CCS detection are shown.
(H) Cellular reactive oxygen species (ROS) were detected using the fluorogenic probe dichlorodihydrofluorescein diacetate (DCFDA) staining in FEA and CRFK cells transfected with siDC7/16 or control siLuc. Data are means ± SEM from at least n = 4 independent experiments. Mann-Whitney test, *$p \leq 0.05$, **$p \leq 0.01$.
(I) ATP quantification in FEA and CRFK cells transfected with either siDC16 or siDC7/16 or siLuc as a control. ATP assay was performed 24 h post-transfection, n = 3 independent experiments. One-way ANOVA with Dunnett's multiple comparisons test, ns, non-significant.

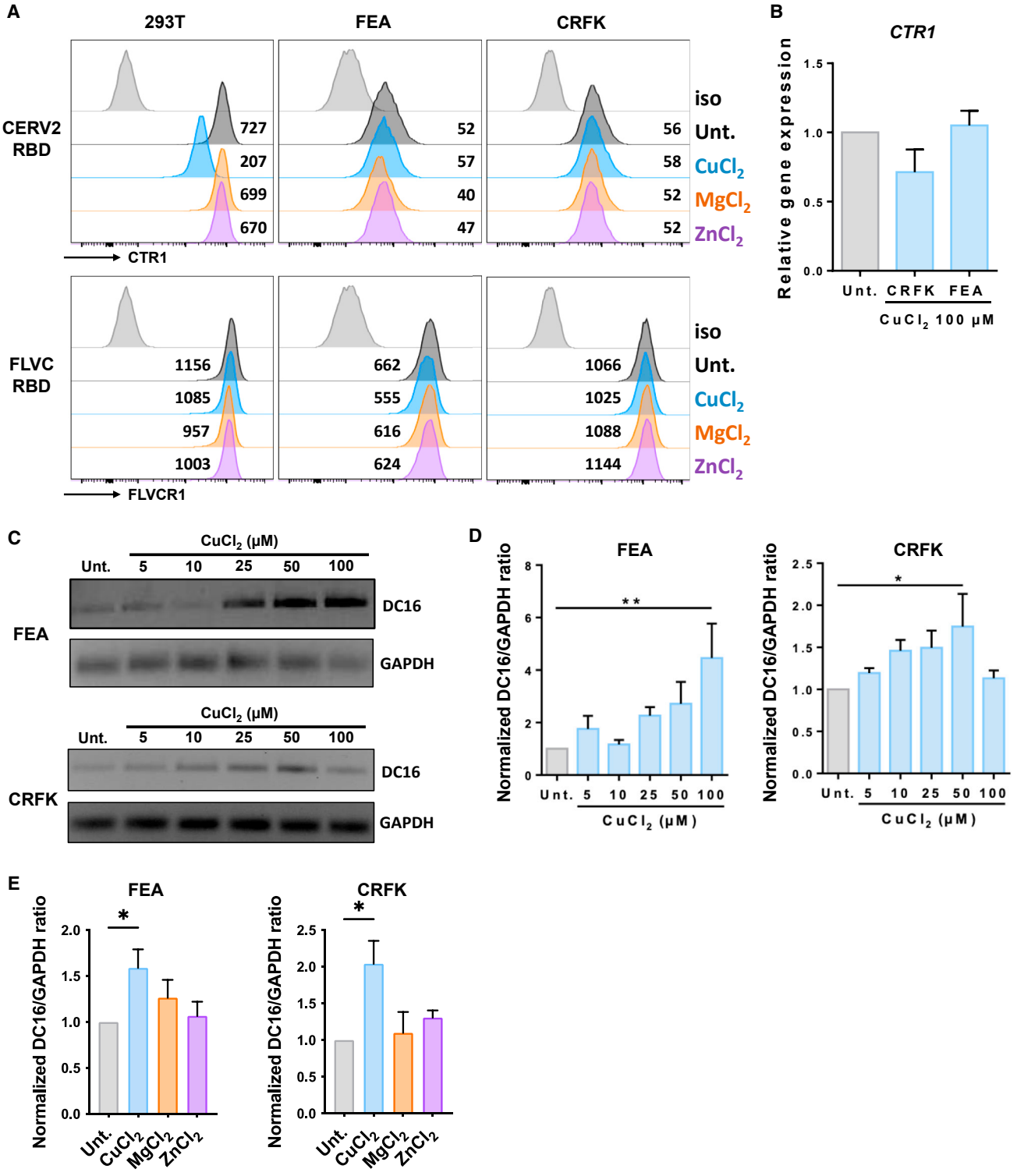

Figure 5. Refrex1 expression is modulated by extracellular copper level

(A) 293T and feline FEA and CRFK cells were either untreated (Unt.) or incubated overnight with 100 μM $CuCl_2$, 100 μM $MgCl_2$, or 100 μM $ZnCl_2$ and evaluated for CTR1 cell-surface expression by flow cytometry using CERV2RBD ligand. Numbers indicate the specific change in mean fluorescence intensity compared with non-specific mock staining (gray histogram) of a representative experiment (n = 3 biological replicates).

(B) Evaluation by qRT-PCR of *CTR1* expression relative to *GAPDH* in feline FEA and CRFK cells incubated overnight with 100 μM copper.

(legend continued on next page)

lower level of copper in human cells overexpressing Refrex1. Conversely, downmodulation of Refrex1 expression in feline cells led to a significant increase in copper levels, which in turn affected the expression of several genes involved in copper homeostasis. Surprisingly, Refrex1 behaves as an essential gene, since we discovered that its downmodulation severely impaired cell survival, implicating Refrex1 as a key regulator of both cellular copper level and toxicity. This copper-induced cell death was associated with significant increased ROS production and apoptosis levels, and further studies are required to uncover the underlying mechanisms. Thus, co-option of Refrex1 that occurred during cat evolution represents an additional layer of CTR1 regulation for the control of cellular copper homeostasis and redox fitness.

We observed a strong inhibitory activity against ERV-DC14 pseudotype infection in the serum of domestic cats, suggesting that plasma-resident Refrex1 can interact with cell-surface CTR1, and this in nearly all cells of the cat organism. Red blood cells (RBCs) are the major constituent of blood cells, and they rely on a proper copper balance to control oxidative stress generated by the high-oxygen environment and by their heme-iron-rich content. They are very sensitive to high copper levels, leading to ROS production, to reduced antioxidant status, and ultimately to hemolysis.[42,43] This suggests that highly regulated copper transport mechanisms exist on the surface of RBCs, and, consistent with this hypothesis, we detected the presence of CTR1 on human RBCs using our DC14RBD ligand.[34] Surprisingly, CTR1 was not detected on feline RBCs (Figure 7C). This is not due to the inability of DC14RBD to recognize the feline CTR1, since it is clearly detected when overexpressed on CHO cells.[34] This may rather be the consequence of CTR1 saturation by Refrex1 present in the serum or secreted by the RBCs during staining. It remains to be determined whether saturation of CTR1 on feline RBCs by soluble Refrex1 from blood can lead to copper transport modulation, as described in cat cell lines (Figure 4E) and as reported with other soluble retroviral Envs on phosphate and glucose transport.[24,25]

In human cells, elevated copper levels trigger the endocytosis of CTR1 from the plasma membrane[3,44] via the retromer-recycling function,[45] which prevents excessive copper uptake and toxic accumulation in cells. We found that this mechanistic adaptation does not occur in feline cells, but we discovered that CTR1 could be regulated in a different way with the help of Refrex1. In cells, Refrex1 is transported through the secretory pathway and is therefore not in contact with cytosolic copper, eliminating a role for Refrex1 in sequestering or carrying copper just after entry via CTR1. In contrast, Refrex1 is known to restrict virus entry through receptor interaction,[16] either by trapping CTR1 in the endoplasmic reticulum, where they can interact with each other before reaching the plasma membrane, or by saturating CTR1 at the plasma membrane. This is reminiscent of a mechanism known as interference with superinfection,[22,46,47] by which chronically infected cells become resistant to exogenous retroviruses through Env-receptor interaction. This interference phenomenon is often accompanied by a defect in SLC function, as exemplified by the phosphate transporters SLC20A1 and SLC20A2, which are affected in their phosphate transport function in the presence of gibbon ape leukemia virus and amphotropic MLV Envs, respectively.[48–50] In the present study, we show that Refrex1 is unable to trap CTR1 in cells and does not have the capacity to induce CTR1 degradation (Figure S3). It is therefore likely that the defect in CTR1-mediated copper transport is due to CTR1 saturation by Refrex1 at the plasma membrane. Surprisingly, we found that Refrex1 expression was transcriptionally upregulated in response to high levels of extracellular copper. This upregulation could result from the promoter activity of the ERV-DC7 or 16 long terminal repeat (LTR)[51] or from an additional promoter of cellular origin. Interestingly, activation of the HERV LTR by copper has already been reported, but the underlying mechanisms of copper action are not known.[52] Overall, our results suggest that cat cells can sense elevated copper levels and respond by stimulating Refrex1 expression and by decreasing CTR1 transport activity in a Refrex1-dependent manner, although we cannot exclude an additional copper-independent role of Refrex1 in cell survival.

KO mouse models of CTR1 have shown an embryonic lethality suggesting that CTR1 defect is lethal in humans as well.[53] So far, only one study has reported a homozygous missense variant of *CTR1* in twin infants associated with neurodegeneration due to brain copper deficiency.[54] Other copper-associated diseases have been reported, two of them involving copper pumps. Indeed, mutations in the *ATP7A* gene are associated with Menkes disease, a disorder of copper deficiency,[55] and mutations in the *ATP7B* gene cause Wilson disease, characterized by copper overload mainly in the liver, but also in other tissues such as the brain.[56] In both cases, pathological mutations lead to copper imbalance with toxic consequences. We demonstrate here that Refrex1 is a key player of cellular copper homeostasis by regulating copper entry mediated by CTR1, and like CTR1, ATP7A, and ATP7B, Refrex1 integrity is crucial for cell physiology and survival. Copper disorders have been reported in several cats, some of which presented mutations in *ATP7B*.[57–59] Likewise, mutations in ERV-DC7 or ERV-DC16 affecting Refrex1 expression or interaction with CTR1 may be associated with cat copper diseases, and as such, *ERV-DC7/16* should be included in the list of candidate genes causing copper disorders in cats.

As reported for Refrex1, the ability of ERV Env to be released in the extracellular environment and to modulate cell metabolism through receptor interaction could be widespread among vertebrates. Such a widespread co-option has been described for syncytins, which play a crucial role in

(C) Evaluation of *DC16* and *GAPDH* gene expression by RT-PCR in feline FEA and CRFK cells incubated overnight with increasing concentrations of copper (5–100 μM). A representative experiment of three is shown.
(D) Quantification of ERV-DC16 expression in cells from (C) expressed as the ratio to *GAPDH* expression. Data are means ± SEM from three independent experiments. One-way ANOVA with Dunnett's multiple comparisons test, *$p \leq 0.05$, **$p \leq 0.01$.
(E) Expression of normalized DC16 expression as in (D) in the presence of 100μM copper, zinc, or magnesium. Data are means ± SEM from three independent experiments. One-way ANOVA with Dunnett's multiple comparisons test, *$p < 0.05$.

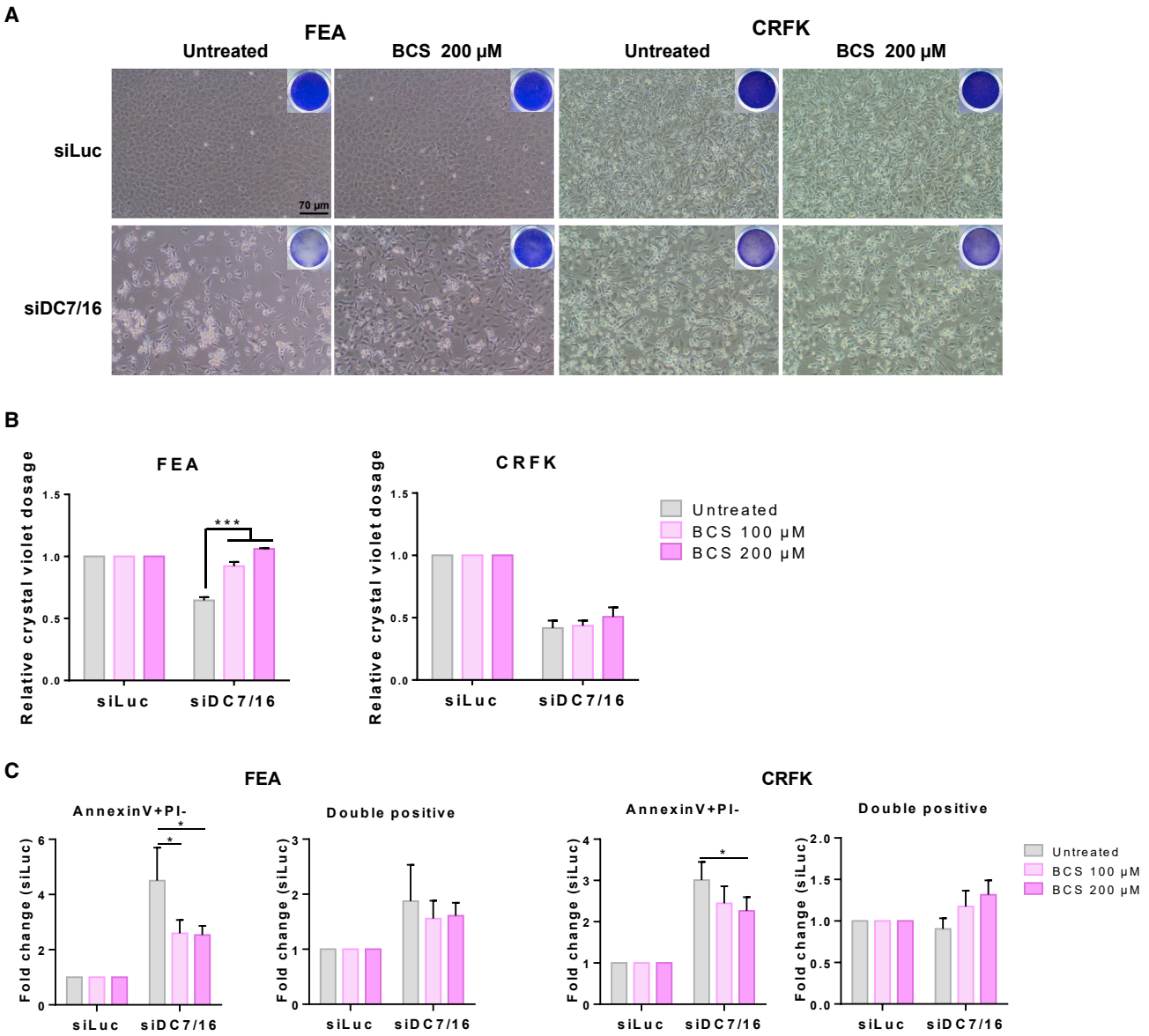

Figure 6. Copper chelator BCS protects Refrex1/DC16-silenced cells from death

FEA and CRFK cells were transfected with siDC7/16 or an siLuc control, and 5 h post-transfection, the medium was replaced with medium containing increasing doses of the copper chelator bathocuproine disulfonate (BCS).

(A) Three days post-transfection, bright-light images were captured and corresponding wells were stained with crystal violet. Representative bright-field images from the untreated and the 200 µM BCS dose cells are shown, and the inset shows the corresponding crystal violet image of the whole well. Scale bar, 70 µm.

(B) Crystal violet of cells from (A) was solubilized and quantified. Data are means ± SEM from n = 3 independent experiments. One-way ANOVA with Dunnett's multiple comparisons test, ***$p \leq 0.001$.

(C) At 24 h post-transfection, cells were stained for Annexin V and propidium iodide (PI). The percentages of cells in the Annexin V^+/PI^- as well as the double-positive quadrant as defined in Figure 2 are shown. Data are means ± SEM from n = 4 or 5 independent experiments. Two-way ANOVA with Dunnett's multiple comparisons test, *$p \leq 0.05$.

placentation in most mammals, as well as marsupials.[13] In domesticated cats, FeLIX is another example of a soluble Env found in cat serum with receptor-binding capacity.[60] FeLIX has been studied only for its role as a facilitator of FeLV-T infection,[27,61,62] but its ability to interact with the feline phosphate transporter SLC20A1 makes it a potential modulator of phosphate influx and metabolism. Two other captured retroviral Envs known to be secreted in the extracellular environment have been identified in humans. These include the HERV-R Env expressed from the *erv3* locus, which contains a stop codon before the transmembrane domain of the TM subunit.[63] This Env is thus non-fusogenic, but retains an intact surface unit (SU) with receptor-binding capacity, although 1% of Caucasian individuals have maintained a shorter Env looking

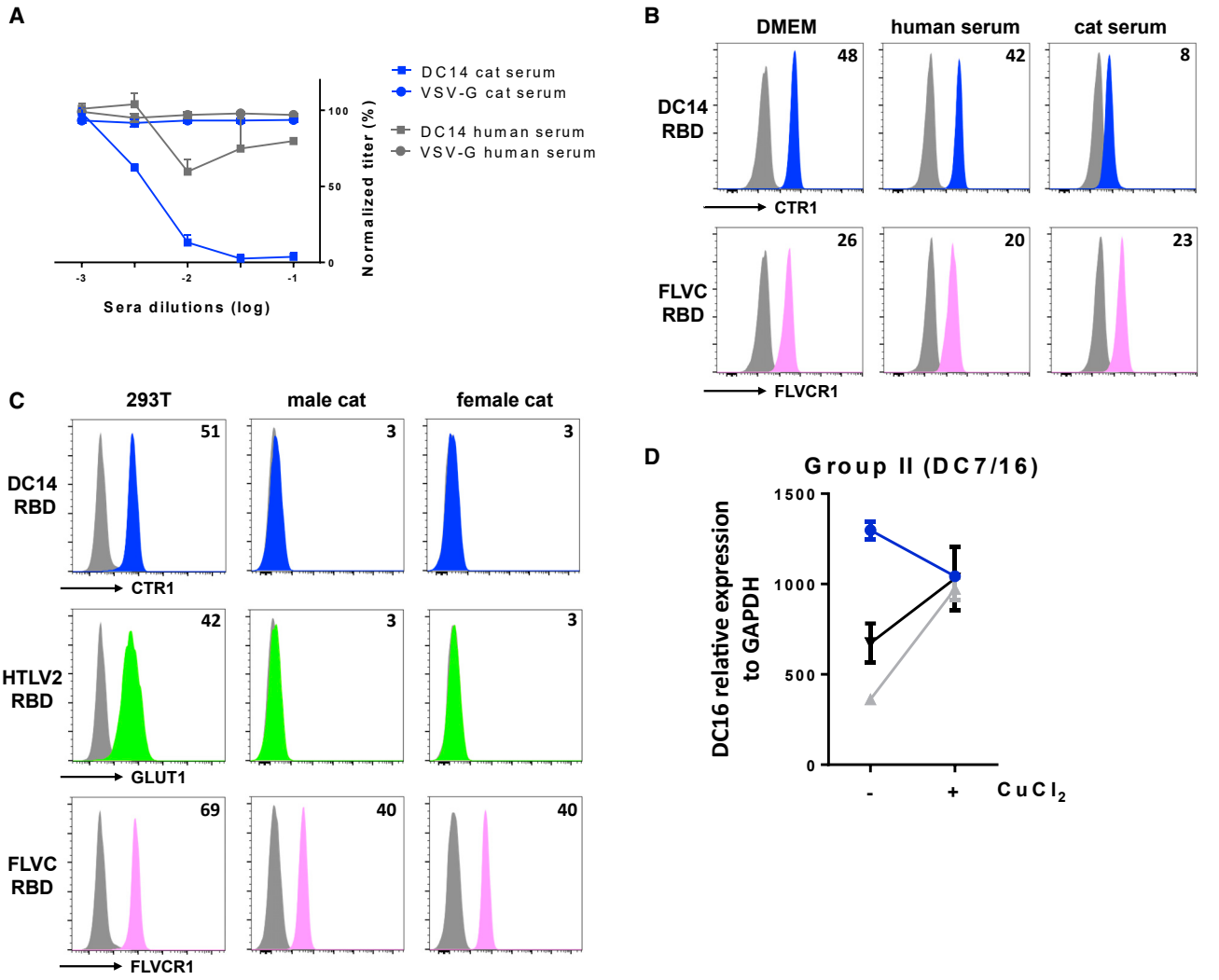

Figure 7. Refrex1 is present in cat serum

(A) 293T cells were incubated overnight with various dilutions of human and cat sera and evaluated for their sensitivity to infection by EGFP lentiviral vector pseudotyped with ERV-DC14 or VSV-G Env. Data are means ± SEM from n = 3 independent experiments.

(B) Evaluation of cell-surface expression of FLVCR1 and CTR1 on 293T cells incubated overnight with human and cat serum dilutions (1:50) by flow cytometry using the indicated RBD ligands. Numbers indicate the specific change in mean fluorescence intensity compared with non-specific mock staining (gray histogram) of a representative experiment (n = 3 biological replicates).

(C) Evaluation of cell-surface expression of FLVCR1, GLUT1, and CTR1 on human and cat red blood cells by flow cytometry using RBD ligands. Binding on 293T is shown as a control. Numbers indicate the specific change in mean fluorescence intensity compared with non-specific mock staining (gray histogram) of a representative experiment (n = 3 biological replicates).

(D) Evaluation by qRT-PCR of ERV-DC16 *env* expression normalized with *GAPDH* in cat PBMCs isolated from whole blood of three independent male cats and incubated overnight in 250 μM $CuCl_2$.

like an RBD.[64] HEMO is another captured Env expressed from an ancestral *env* gene with an intact open reading frame.[65] Surprisingly, although HEMO is expressed as an integral envelope glycoprotein, its SU is shed in the extracellular environment and found at high levels in the blood circulation of pregnant women.[65] Thus, the expression of soluble Envs from co-opted ERV genes is not limited to Refrex1 and appears to exist in other organisms. Further studies are required to identify cellular partners of these soluble ERV factors to evaluate their roles in physiological metabolic pathways and in metabolic disorders.

Limitations of the study

Our study has limitations that should be considered. First, we were confronted with a lack of tools such as antibodies for detection of feline proteins. For example, although we could observe upregulation of *Refrex1* mRNA in the presence of elevated extracellular copper, we could not confirm that this is translated into protein increase. In the same line, the silencing of *Refrex1* by siDC16 transfection of FEA and CRFK cells was monitored by qRT-PCR, but we could not show Refrex1 protein depletion. We were also unable to document endogenous expression of feline

CTR1 proteins at the global level or at the plasma membrane of cat cells using antibodies, and we could only use an overexpression system to observe that feline CTR1 is not degraded nor retained into cells by Refrex1. Second, we demonstrated the role played by Refrex1 in the control of cellular copper homeostasis, but the underlying mechanism, which we think is at the copper entry level through CTR1, requires further investigations with ^{64}Cu-uptake experiments. However, we could not perform these experiments, considering the extremely short half-life of this radioactive compound (12.7 h). Finally, the inability of feline cells to undergo CTR1 endocytosis in copper-excess conditions despite intrinsically competent feline CTR1 remains to be further investigated to understand why modern cats have evolutionarily conserved Refrex1 as a negative regulator of CTR1-mediated copper uptake. It will be useful to gain access to feline species samples that do not express Refrex1 to compare with Refrex1-positive modern cats and identify differences in total cellular copper and in the capacity of adaptation to copper excess, like CTR1 endocytosis.

STAR★METHODS

Detailed methods are provided in the online version of this paper and include the following:

- KEY RESOURCES TABLE
- RESOURCE AVAILABILITY
  - Lead contact
  - Materials availability
  - Data and code availability
- EXPERIMENTAL MODEL AND STUDY PARTICIPANT DETAILS
  - Cell lines
  - Primary cells
- METHOD DETAILS
  - Plasmids
  - Viral productions and infections
  - Monitoring cell surface expression of retroviral receptors/solute carriers using retroviral RBD ligands
  - RNA isolation, synthesis of cDNA, RT-PCR and RT-qPCR
  - Immunoblotting
  - Crystal violet viability staining
  - Copper dosage
  - Viability assay
  - ATP measurement
  - Annexin V/propidium iodide staining
  - ROS staining
  - PBMCs purification
- QUANTIFICATION AND STATISTICAL ANALYSIS

SUPPLEMENTAL INFORMATION

Supplemental information can be found online at https://doi.org/10.1016/j.celrep.2023.113065.

ACKNOWLEDGMENTS

The authors are grateful to the Centre Hospitalier Vétérinaire Languedocia, the Clinique Vétérinaire de l'Aiguelongue, the Clinique Vétérinaire du Corum, and the Clinique Vétérinaire d'Alco in Montpellier, France, for providing blood samples; to the OSU OREME platform of Montpellier University for metal dosage; to Andrea Cimarelli (CIRI, Lyon, France) for CRFK cells; to Dennis J. Thiele (Duke University, NC, USA) for advice; and to Paul Bieniasz (Rockefeller University, New York, NY, USA) for the CERV2 Env plasmid. We also thank all the members of our team for technical help and advice. This work was supported by the French National Research Agency (ANR CALCIPHOS/ANR-17-CE14-0008-01 to J.-L.B.) and by the French SIDACTION (19-2-AEQ-12560 to J.-L.B.). S.T. was supported by the ANR CALCIPHOS, L.C. by the French AIDS National Research Agency ANRS (ECTZ134113), V.C. by CNRS, and J.-L.B. by INSERM.

AUTHOR CONTRIBUTIONS

Conceptualization, S.T., L.C., V.C., and J.-L.B.; methodology, S.T., L.C., V.C., and J.-L.B.; investigation, S.T., L.C., A.L., V.C., and J.-L.B.; writing – original draft, J.-L.B.; visualization, S.T. and L.C.; writing – review & editing, S.T., L.C., V.C., and J.-L.B.; funding acquisition, J.-L.B.; resources, V.C. and J.-L.B.; supervision, V.C. and J.-L.B.

DECLARATION OF INTERESTS

The authors declare no competing interests.

Received: August 8, 2022
Revised: June 14, 2023
Accepted: August 21, 2023
Published: September 7, 2023

REFERENCES

1. Peña, M.M., Lee, J., and Thiele, D.J. (1999). A Delicate Balance: Homeostatic Control of Copper Uptake and Distribution. J. Nutr. *129*, 1251–1260. https://doi.org/10.1093/jn/129.7.1251.
2. Kim, B.-E., Nevitt, T., and Thiele, D.J. (2008). Mechanisms for copper acquisition, distribution and regulation. Nat. Chem. Biol. *4*, 176–185. https://doi.org/10.1038/nchembio.72.
3. Petris, M.J., Smith, K., Lee, J., and Thiele, D.J. (2003). Copper-stimulated endocytosis and degradation of the human copper transporter, hCtr1. J. Biol. Chem. *278*, 9639–9646. https://doi.org/10.1074/jbc.M209455200.
4. Öhrvik, H., Logeman, B., Turk, B., Reinheckel, T., and Thiele, D.J. (2016). Cathepsin Protease Controls Copper and Cisplatin Accumulation via Cleavage of the Ctr1 Metal-binding Ectodomain. J. Biol. Chem. *291*, 13905–13916. https://doi.org/10.1074/jbc.M116.731281.
5. Öhrvik, H., Nose, Y., Wood, L.K., Kim, B.-E., Gleber, S.-C., Ralle, M., and Thiele, D.J. (2013). Ctr2 regulates biogenesis of a cleaved form of mammalian Ctr1 metal transporter lacking the copper- and cisplatin-binding ectodomain. Proc. Natl. Acad. Sci. USA *110*, E4279–E4288. https://doi.org/10.1073/pnas.1311749110.
6. Logeman, B.L., Wood, L.K., Lee, J., and Thiele, D.J. (2017). Gene duplication and neo-functionalization in the evolutionary and functional divergence of the metazoan copper transporters Ctr1 and Ctr2. J. Biol. Chem. *292*, 11531–11546. https://doi.org/10.1074/jbc.M117.793356.
7. Hayward, A., Cornwallis, C.K., and Jern, P. (2015). Pan-vertebrate comparative genomics unmasks retrovirus macroevolution. Proc. Natl. Acad. Sci. USA *112*, 464–469. https://doi.org/10.1073/pnas.1414980112.
8. Lander, E.S., Linton, L.M., Birren, B., Nusbaum, C., Zody, M.C., Baldwin, J., Devon, K., Dewar, K., Doyle, M., Fitzhugh, W., et al. (2001). Correction: Initial sequencing and analysis of the human genome. Nature *412*, 565–566. https://doi.org/10.1038/35087627.
9. Dewannieux, M., and Heidmann, T. (2013). Endogenous retroviruses: acquisition, amplification and taming of genome invaders. Curr. Opin. Virol. *3*, 646–656. https://doi.org/10.1016/j.coviro.2013.08.005.

10. Wang, J., and Han, G.-Z. (2020). Frequent Retroviral Gene Co-option during the Evolution of Vertebrates. Mol. Biol. Evol. *37*, 3232–3242. https://doi.org/10.1093/molbev/msaa180.

11. Villesen, P., Aagaard, L., Wiuf, C., and Pedersen, F.S. (2004). Identification of endogenous retroviral reading frames in the human genome. Retrovirology *1*, 32-13. https://doi.org/10.1186/1742-4690-1-32.

12. Blaise, S., de Parseval, N., and Heidmann, T. (2005). Functional characterization of two newly identified human endogenous retrovirus coding envelope genes. Retrovirology *2*, 19-11. https://doi.org/10.1186/1742-4690-2-19.

13. Lavialle, C., Cornelis, G., Dupressoir, A., Esnault, C., Heidmann, O., Vernochet, C., and Heidmann, T. (2013). Paleovirology of "syncytins". Philos. Trans. R. Soc. Lond. B Biol. Sci. *368*, 20120507. https://doi.org/10.1098/rstb.2012.0507.

14. Buller, R.S., Sitbon, M., and Portis, J.L. (1988). The endogenous mink cell focus-forming (MCF) gp70 linked to the Rmcf gene restricts MCF virus replication in vivo and provides partial resistance to erythroleukemia induced by Friend murine leukemia virus. J. Exp. Med. *167*, 1535–1546. https://doi.org/10.1084/jem.167.5.1535.

15. Ikeda, H., Laigret, F., Martin, M.A., and Repaske, R. (1985). Characterization of a molecularly cloned retroviral sequence associated with Fv-4 resistance. J. Virol. *55*, 768–777. https://doi.org/10.1128/jvi.55.3.768-777.1985.

16. Ito, J., Watanabe, S., Hiratsuka, T., Kuse, K., Odahara, Y., Ochi, H., Kawamura, M., and Nishigaki, K. (2013). Refrex-1, a Soluble Restriction Factor against Feline Endogenous and Exogenous Retroviruses. J. Virol. *87*, 12029–12040. https://doi.org/10.1128/JVI.01267-13.

17. Blanco-Melo, D., Gifford, R.J., and Bieniasz, P.D. (2017). Co-option of an endogenous retrovirus envelope for host defense in hominid ancestors. Elife *6*, e22519–19. https://doi.org/10.7554/eLife.22519.

18. Kozak, C.A. (2014). Origins of the Endogenous and Infectious Laboratory Mouse Gammaretroviruses. Viruses *7*, 1–26. https://doi.org/10.3390/v7010001.

19. Mi, S., Lee, X., Li, X., Veldman, G.M., Finnerty, H., Racie, L., LaVallie, E., Tang, X.-Y., Edouard, P., Howes, S., et al. (2000). Syncytin is a captive retroviral envelope protein involved in human placental morphogenesis. Nature *403*, 785–789. https://doi.org/10.1038/35001608.

20. Blaise, S., de Parseval, N., Bénit, L., and Heidmann, T. (2003). Genomewide screening for fusogenic human endogenous retrovirus envelopes identifies syncytin 2, a gene conserved on primate evolution. Proc. Natl. Acad. Sci. USA *100*, 13013–13018. https://doi.org/10.1073/pnas.2132646100.

21. Wang, T., Medynets, M., Johnson, K.R., Doucet-O'Hare, T.T., DiSanza, B., Li, W., Xu, Y., Bagnell, A., Tyagi, R., Sampson, K., et al. (2020). Regulation of stem cell function and neuronal differentiation by HERV-K via mTOR pathway. Proc. Natl. Acad. Sci. USA *117*, 17842–17853. https://doi.org/10.1073/pnas.2002427117.

22. Overbaugh, J., Miller, A.D., and Eiden, M.V. (2001). Receptors and entry cofactors for retroviruses include single and multiple transmembrane-spanning proteins as well as newly described glycophosphatidylinositol-anchored and secreted proteins. Microbiol. Mol. Biol. Rev. *65*, 371–389, , table of contents, table of contents. https://doi.org/10.1128/MMBR.65.3.371-389.

23. Rasko, J.E., Battini, J.L., Gottschalk, R.J., Mazo, I., and Miller, A.D. (1999). The RD114/simian type D retrovirus receptor is a neutral amino acid transporter. Proc. Natl. Acad. Sci. USA *96*, 2129–2134. https://doi.org/10.1073/pnas.96.5.2129.

24. Manel, N., Kim, F.J., Kinet, S., Taylor, N., Sitbon, M., and Battini, J.-L. (2003). The Ubiquitous Glucose Transporter GLUT-1 Is a Receptor for HTLV. Cell *115*, 449–459. https://doi.org/10.1016/S0092-8674(03)00881-X.

25. Giovannini, D., Touhami, J., Charnet, P., Sitbon, M., and Battini, J.-L. (2013). Inorganic Phosphate Export by the Retrovirus Receptor XPR1 in Metazoans. Cell Rep. *3*, 1866–1873. https://doi.org/10.1016/j.celrep.2013.05.035.

26. Mendoza, R., Miller, A.D., and Overbaugh, J. (2013). Disruption of Thiamine Uptake and Growth of Cells by Feline Leukemia Virus Subgroup A. J. Virol. *87*, 2412–2419. https://doi.org/10.1128/JVI.03203-12.

27. Anderson, M.M., Lauring, A.S., Burns, C.C., and Overbaugh, J. (2000). Identification of a Cellular Cofactor Required for Infection by Feline Leukemia Virus. Science *287*, 1828–1830. https://doi.org/10.1126/science.287.5459.1828.

28. Sarma, P.S., and Log, T. (1973). Subgroup classification of feline leukemia and sarcoma viruses by viral interference and neutralization tests. Virology *54*, 160–169. https://doi.org/10.1016/0042-6822(73)90125-6.

29. Takeuchi, Y., Vile, R.G., Simpson, G., O'Hara, B., Collins, M.K., and Weiss, R.A. (1992). Feline leukemia virus subgroup B uses the same cell surface receptor as gibbon ape leukemia virus. J. Virol. *66*, 1219–1222. https://doi.org/10.1128/jvi.66.2.1219-1222.1992.

30. Anai, Y., Ochi, H., Watanabe, S., Nakagawa, S., Kawamura, M., Gojobori, T., and Nishigaki, K. (2012). Infectious Endogenous Retroviruses in Cats and Emergence of Recombinant Viruses. J. Virol. *86*, 8634–8644. https://doi.org/10.1128/JVI.00280-12.

31. Ngo, M.H., Arnal, M., Sumi, R., Kawasaki, J., Miyake, A., Grant, C.K., Otoi, T., Fernández de Luco, D., and Nishigaki, K. (2019). Tracking the Fate of Endogenous Retrovirus Segregation in Wild and Domestic Cats. J. Virol. *93*, 013244-19–e1419. https://doi.org/10.1128/JVI.01324-19.

32. Kawasaki, J., and Nishigaki, K. (2018). Tracking the Continuous Evolutionary Processes of an Endogenous Retrovirus of the Domestic Cat: ERV-DC. Viruses *10*, 179. https://doi.org/10.3390/v10040179.

33. Ito, J., Baba, T., Kawasaki, J., and Nishigaki, K. (2016). Ancestral Mutations Acquired in Refrex-1, a Restriction Factor against Feline Retroviruses, during its Cooption and Domestication. J. Virol. *90*, 1470–1485. https://doi.org/10.1128/JVI.01904-15.

34. Tury, S., Giovannini, D., Ivanova, S., Touhami, J., Courgnaud, V., and Battini, J.-L. (2022). Identification of Copper Transporter 1 as a Receptor for Feline Endogenous Retrovirus ERV-DC14. J. Virol. *96*, e0022922. https://doi.org/10.1128/jvi.00229-22.

35. Miyake, A., Ngo, M.H., Wulandari, S., Shimojima, M., Nakagawa, S., Kawasaki, J., and Nishigaki, K. (2022). Convergent evolution of antiviral machinery derived from endogenous retrovirus truncated envelope genes in multiple species. Proc. Natl. Acad. Sci. USA *119*, e2114441119. https://doi.org/10.1073/pnas.2114441119.

36. Ursini, F., and Maiorino, M. (2020). Lipid peroxidation and ferroptosis: The role of GSH and GPx4. Free Radic. Biol. Med. *152*, 175–185. https://doi.org/10.1016/j.freeradbiomed.2020.02.027.

37. Soll, S.J., Neil, S.J.D., and Bieniasz, P.D. (2010). Identification of a receptor for an extinct virus. Proc. Natl. Acad. Sci. USA *107*, 19496–19501. https://doi.org/10.1073/pnas.1012344107.

38. Miller, A.D., and Rosman, G.J. (1989). Improved retroviral vectors for gene transfer and expression. Biotechniques 7, 989–990. 980–2, 984-6, 989-90, 984–986,.

39. Bertinato, J., Iskandar, M., and L'Abbé, M.R. (2003). Copper Deficiency Induces the Upregulation of the Copper Chaperone for Cu/Zn Superoxide Dismutase in Weanling Male Rats. J. Nutr. *133*, 28–31. https://doi.org/10.1093/jn/133.1.28.

40. Prohaska, J.R., Broderius, M., and Brokate, B. (2003). Metallochaperone for Cu,Zn-superoxide dismutase (CCS) protein but not mRNA is higher in organs from copper-deficient mice and rats. Arch. Biochem. Biophys. *417*, 227–234. https://doi.org/10.1016/S0003-9861(03)00364-3.

41. Ishida, S., Andreux, P., Poitry-Yamate, C., Auwerx, J., and Hanahan, D. (2013). Bioavailable copper modulates oxidative phosphorylation and growth of tumors. Proc. Natl. Acad. Sci. USA *110*, 19507–19512. https://doi.org/10.1073/pnas.1318431110.

42. Attri, S., Sharma, N., Jahagirdar, S., Thapa, B.R., and Prasad, R. (2006). Erythrocyte Metabolism and Antioxidant Status of Patients with Wilson

Disease with Hemolytic Anemia. Pediatr. Res. *59*, 593–597. https://doi.org/10.1203/01.pdr.0000203098.77573.39.

43. Clopton, D.A., and Saltman, P. (1997). Copper-specific damage in human erythrocytes exposed to oxidative stress. Biol. Trace Elem. Res. *56*, 231–240. https://doi.org/10.1007/BF02785396.
44. Kar, S., Sen, S., Maji, S., Saraf, D., Ruturaj, R., Paul, R., Dutt, S., Mondal, B., Rodriguez-Boulan, E., Schreiner, R., et al. (2022). Copper(II) import and reduction are dependent on His-Met clusters in the extracellular amino terminus of human copper transporter-1. J. Biol. Chem. *298*, 101631. https://doi.org/10.1016/j.jbc.2022.101631.
45. Curnock, R., and Cullen, P.J. (2020). Mammalian copper homeostasis requires retromer-dependent recycling of the high-affinity copper transporter 1. J. Cell Sci. *133*, jcs249201. https://doi.org/10.1242/jcs.249201.
46. Weiss, R.A. (1993). Cellular receptors and viral glycoproteins involved in retroviral entry. In The Retroviridae, J. Levy, ed. (Plenum Press), pp. 1–108.
47. Miller, A.D., and Wolgamot, G. (1997). Murine retroviruses use at least six different receptors for entry into Mus dunni cells. J. Virol. *71*, 4531–4535. https://doi.org/10.1128/jvi.71.6.4531-4535.1997.
48. Kavanaugh, M.P., Miller, D.G., Zhang, W., Law, W., Kozak, S.L., Kabat, D., and Miller, A.D. (1994). Cell-surface receptors for gibbon ape leukemia virus and amphotropic murine retrovirus are inducible sodium-dependent phosphate symporters. Proc. Natl. Acad. Sci. USA *91*, 7071–7075. https://doi.org/10.1073/pnas.91.15.7071.
49. Olah, Z., Lehel, C., Anderson, W.B., Eiden, M.V., and Wilson, C.A. (1994). The cellular receptor for gibbon ape leukemia virus is a novel high affinity sodium-dependent phosphate transporter. J. Biol. Chem. *269*, 25426–25431. https://doi.org/10.1016/S0021-9258(18)47267-5.
50. Wilson, C.A., Eiden, M.V., Anderson, W.B., Lehel, C., and Olah, Z. (1995). The dual-function hamster receptor for amphotropic murine leukemia virus (MuLV), 10A1 MuLV, and gibbon ape leukemia virus is a phosphate symporter. J. Virol. *69*, 534–537. https://doi.org/10.1128/jvi.69.1.534-537.1995.
51. Kuse, K., Ito, J., Miyake, A., Kawasaki, J., Watanabe, S., Makundi, I., Ngo, M.H., Otoi, T., and Nishigaki, K. (2016). Existence of Two Distinct Infectious Endogenous Retroviruses in Domestic Cats and Their Different Strategies for Adaptation to Transcriptional Regulation. J. Virol. *90*, 9029–9045. https://doi.org/10.1128/JVI.00716-16.
52. Karimi, A., Sheervalilou, R., and Kahroba, H. (2019). A New Insight on Activation of Human Endogenous Retroviruses (HERVs) in Malignant Melanoma upon Exposure to CuSO4. Biol. Trace Elem. Res. *191*, 70–74. https://doi.org/10.1007/s12011-018-1605-6.
53. Lee, J., Prohaska, J.R., and Thiele, D.J. (2001). Essential role for mammalian copper transporter Ctr1 in copper homeostasis and embryonic development. Proc. Natl. Acad. Sci. USA *98*, 6842–6847. https://doi.org/10.1073/pnas.111058698.
54. Batzios, S., Tal, G., DiStasio, A.T., Peng, Y., Charalambous, C., Nicolaides, P., Kamsteeg, E.-J., Korman, S.H., Mandel, H., Steinbach, P.J., et al. (2022). Newly identified disorder of copper metabolism caused by variants in CTR1, a high-affinity copper transporter. Hum. Mol. Genet. *31*, 4121–4130. https://doi.org/10.1093/hmg/ddac156.
55. Tümer, Z. (2013). An overview and update of ATP7A mutations leading to Menkes disease and occipital horn syndrome. Hum. Mutat. *34*, 417–429. https://doi.org/10.1002/humu.22266.
56. Członkowska, A., Litwin, T., Dusek, P., Ferenci, P., Lutsenko, S., Medici, V., Rybakowski, J.K., Weiss, K.H., and Schilsky, M.L. (2018). Wilson disease. Nat. Rev. Dis. Prim. *4*, 21. https://doi.org/10.1038/s41572-018-0018-3.
57. Meertens, N.M., Bokhove, C.A.M., and van den Ingh, T.S.G.A.M. (2005). Copper-associated Chronic Hepatitis and Cirrhosis in a European Shorthair Cat. Vet. Pathol. *42*, 97–100. https://doi.org/10.1354/vp.42-1-97.
58. Asada, H., Chambers, J.K., Kojima, M., Goto-Koshino, Y., Nakagawa, T., Yokoyama, N., Tsuboi, M., Uchida, K., Tsujimoto, H., and Ohno, K. (2020). Variations in ATP7B in cats with primary copper-associated hepatopathy. J. Feline Med. Surg. *22*, 753–759. https://doi.org/10.1177/1098612X19884763.
59. Asada, H., Kojima, M., Nagahara, T., Goto-Koshino, Y., Chambers, J.K., Nakagawa, T., Yokoyama, N., Uchida, K., Tsujimoto, H., and Ohno, K. (2019). Hepatic copper accumulation in a young cat with familial variations in the ATP7B gene. J. Vet. Intern. Med. *33*, 874–878. https://doi.org/10.1111/jvim.15399.
60. Sakaguchi, S., Shojima, T., Fukui, D., and Miyazawa, T. (2015). A soluble envelope protein of endogenous retrovirus (FeLIX) present in serum of domestic cats mediates infection of a pathogenic variant of feline leukemia virus. J. Gen. Virol. *96*, 681–687. https://doi.org/10.1099/vir.0.071688-0.
61. Lauring, A.S., Anderson, M.M., and Overbaugh, J. (2001). Specificity in Receptor Usage by T-Cell-Tropic Feline Leukemia Viruses: Implications for the In Vivo Tropism of Immunodeficiency-Inducing Variants. J. Virol. *75*, 8888–8898. https://doi.org/10.1128/jvi.75.19.8888-8898.2001.
62. Cheng, H.H., Anderson, M.M., and Overbaugh, J. (2007). Feline leukemia virus T entry is dependent on both expression levels and specific interactions between cofactor and receptor. Virology *359*, 170–178. https://doi.org/10.1016/j.virol.2006.09.004.
63. O'Connell, C., O'Brien, S., Nash, W.G., and Cohen, M. (1984). ERV3, a full-length human endogenous provirus: chromosomal localization and evolutionary relationships. Virology *138*, 225–235. https://doi.org/10.1016/0042-6822(84)90347-7.
64. de Parseval, N., and Heidmann, T. (1998). Physiological Knockout of the Envelope Gene of the Single-Copy ERV-3 Human Endogenous Retrovirus in a Fraction of the Caucasian Population. J. Virol. *72*, 3442–3445. https://doi.org/10.1128/JVI.72.4.3442-3445.1998.
65. Heidmann, O., Béguin, A., Paternina, J., Berthier, R., Deloger, M., Bawa, O., and Heidmann, T. (2017). HEMO, an ancestral endogenous retroviral envelope protein shed in the blood of pregnant women and expressed in pluripotent stem cells and tumors. Proc. Natl. Acad. Sci. USA *114*, E6642–E6651. https://doi.org/10.1073/pnas.1702204114.
66. Jarrett, O., Laird, H.M., and Hay, D. (1973). Determinants of the host range of feline leukaemia viruses. J. Gen. Virol. *20*, 169–175. https://doi.org/10.1099/0022-1317-20-2-169.
67. Lassaux, A., Sitbon, M., and Battini, J.-L. (2005). Residues in the Murine Leukemia Virus Capsid That Differentially Govern Resistance to Mouse *Fv1* and Human *Ref1* Restrictions. J. Virol. *79*, 6560–6564. https://doi.org/10.1128/JVI.79.10.6560-6564.2005.
68. Battini, J.L., Rasko, J.E., and Miller, A.D. (1999). A human cell-surface receptor for xenotropic and polytropic murine leukemia viruses: possible role in G protein-coupled signal transduction. Proc. Natl. Acad. Sci. USA *96*, 1385–1390. https://doi.org/10.1073/pnas.96.4.1385.
69. Demaison, C., Parsley, K., Brouns, G., Scherr, M., Battmer, K., Kinnon, C., Grez, M., and Thrasher, A.J. (2002). High-level transduction and gene expression in hematopoietic repopulating cells using a human immunodeficiency [correction of imunodeficiency] virus type 1-based lentiviral vector containing an internal spleen focus forming virus promoter. Hum. Gene Ther. *13*, 803–813. https://doi.org/10.1089/10430340252898984.
70. López-Sánchez, U., Tury, S., Nicolas, G., Wilson, M.S., Jurici, S., Ayrignac, X., Courgnaud, V., Saiardi, A., Sitbon, M., and Battini, J.-L. (2020). Interplay between primary familial brain calcification-associated SLC20A2 and XPR1 phosphate transporters requires inositol polyphosphates for control of cellular phosphate homeostasis. J. Biol. Chem. *295*, 9366–9378. https://doi.org/10.1074/jbc.RA119.011376.

STAR★METHODS

KEY RESOURCES TABLE

REAGENT or RESOURCE	SOURCE	IDENTIFIER
Antibodies		
Mouse monoclonal anti-CTR1, clone 1A4H5	Proteintech	Cat#67221-1-Ig; RRID:AB_2882512
Mouse monoclonal anti-FLAG, clone M2	Sigma	Cat#F1804; RRID:AB_262044
Rat monoclonal anti-HA, clone 3F10	Roche	Cat#11867423001; RRID:AB_390918
Rabbit polyclonal anti-CCS	Aviva Systems Biology	Cat# ARP661007
Mouse monoclonal anti ß-actin HRP, clone AC-15	Sigma	Cat#A3854; RRID:AB_262011
Goat anti-mouse IgG1 Alexa Fluor 488	ThermoFisher	Cat#A21121; RRID:AB_2535764
Goat anti-rat IgG HRP	Sigma	Cat#A9037; RRID:AB_258429
Donkey anti-mouse IgG HRP	Jackson	Cat#715-035-150; RRID:AB_2340770
Goat anti-mouse IgG1 Alexa Fluor 647	ThermoFisher	Cat#A-21240; RRID:AB_2535809
Bacterial and virus strains		
DH5-alpha Competent *E. coli*	New England Bioloabs	Cat#C2987H
Biological samples		
Domestic cat blood samples	Centre Hospitalier Vétérinaire Languedocia, Clinique vétérinaire de l'Aiguelongue, Clinique vétérinaire du Corum, Clinique vétérinaires d'Alco, Montpellier, France	N/A
Chemicals, peptides, and recombinant proteins		
CuCl2	Sigma	Cat#307483
MgCl2	Sigma	Cat#208367
ZnCl2	Sigma	Cat#Z0152-50G
Luminata Forte detection reagent	Merck Millipore	Cat#ELLUF0100
Complete Protease inhibitor cocktail	Roche/Merck	Cat#4 693 132 001
JetPrime	Polyplus	Cat#101000046
Bathocuproine disulfonic acid (BCS)	Sigma	Cat#146625-1G
Formaline	Sigma	Cat#HT5011
Crystal violet	Sigma	Cat#C6158-50G
Pierce™ IP lysis buffer	ThermoFisher	Cat#87788
HNO3 5%	Sigma	Cat#84378
H2DCFDA	ThermoFisher	Cat#D399
SYTOX Red	ThermoFisher	Cat#S34859
Histopaque	Sigma	Cat#11191
Critical commercial assays		
RNeasy Plus Mini Kit	Qiagen	Cat#74134
Superscript II First Strand Synthesis System	Invitrogen	Cat#11904018
One Taq DNA Polymerase	New England Biolabs	Cat#M0480
PCR clean-up Gel Extraction kit	Macherey Nagel	Cat#740609.50
Luna Cell Ready Lysis Module	New England Biolabs	Cat#E3032S
Luna One-Step RT-qPCR Kit	New England Biolabs	Cat#M300
Pierce™ BCA protein assay kit	ThermoFisher	Cat#23225
CellTiter 96® AQueous One Solution Cell Proliferation Assay	Promega	Cat#G3582
ATPlite Luminescence Assay System	PerkinElmer	Cat#6016941
KIT NUCLEOBOND PC 100	MACHEREY-NAGEL	Cat#740573-20

(*Continued on next page*)

Continued

REAGENT or RESOURCE	SOURCE	IDENTIFIER
eBioscience Annexin V-FITC Apoptosis detection kit	ThermoFisher	Cat#BMS500FI
PrimeSTAR® Max DNA Polymerase	Takara	Cat# R045A
Experimental models: Cell lines		
Human: HEK (Human Embryonic Kidney) 293T cells	ATCC	Cat#CRL-3216; RRID: CVCL_0063
Human: HEK (Human Embryonic Kidney) 293T CTR1 KO cells	Tury et al, J Virol, 2022[34]	https://doi.org/10.1128/jvi.00229-22
Hamster: CHO-K1 (Chinese Hamster Ovary) cells	ATCC	Cat#CCL-61 ; RRID:CVCL_0213
Domestic cat: FEA (Feline embryonic fibroblast) cells	Jarrett O. et al , 1973[66]	https://doi.org/10.1099/0022-1317-20-2-169 RRID:CVCL_UG17
Domestic cat: CRFK (Crandell feline kidney) cells	ATCC	Cat#CCL94 ; RRID CVCL 2466
Oligonucleotides		
For Oligonucleotides, see Table S1	N/A	N/A
Recombinant DNA		
Plasmid: Cas9-GFP expressing vector pX458	Addgene	Cat#48138
Plasmid: PLXSN	Miller et al, Biotechniques, 1989[38]	PMID: 2631796
Plasmid: PLXSN human CTR1	Tury et al, J Virol, 2022[34]	https://doi.org/10.1128/jvi.00229-22
Plasmid: PLXSN cat CTR1	Tury et al, J Virol, 2022[34]	https://doi.org/10.1128/jvi.00229-22
Plasmid: MLV Gag-Pol expression vector pC57GPBEB	Lassaux et al, , J Virol, 2005[67]	https://doi.org/10.1128/jvi.79.10.6560-6564.2005
Plasmid: VSV-G Env expression vector pCSIG	Battini et al, PNAS, 1999[68]	https://doi.org/10.1073/pnas.96.4.1385
Plasmid: lentiviral transfer plasmid pCSGW	Demaison et al, Human Gene Ther, 2002[69]	https://doi.org/10.1089/10430340252898984
Plasmid: HIV-1 Gag-Pol expression vector psPAX2	Addgene	Cat#12260
Plasmid: ERV-DC14 Env expression vector	Tury et al, J Virol, 2022[34]	https://doi.org/10.1128/jvi.00229-22
Plasmid: ERV-DC16 Env expression vector	This paper	N/A
Plasmid: FeLV-C Env expression vector	Tury et al, J Virol, 2022[34]	https://doi.org/10.1128/jvi.00229-22
Plasmid: ERV-DC14 RBD-IgG1 Fc expression vector	Tury et al, J Virol, 2022[34]	https://doi.org/10.1128/jvi.00229-22
Plasmid: ERV-DC16 RBD-IgG1 Fc expression vector	This paper	N/A
Plasmid: ERV-DC16-HA expresssion vector	This paper	N/A
Plasmid: FeLV-C RBD-IgG1 Fc expression vector	Tury et al, J Virol, 2022[34]	https://doi.org/10.1128/jvi.00229-22
Plasmid: DC14 RBD-IgG1 Fc expression vector	Tury et al, J Virol, 2022[34]	https://doi.org/10.1128/jvi.00229-22
Plasmid: Amphotropic-MLV RBD-IgG1 Fc expression vector	Manel et al, Cell, 2003[24]	https://doi.org/10.1016/s0092-8674(03)00881-x
Plasmid: CERV2 Env expression vector	Soll et al, PNAS, 2010[37]	https://doi.org/10.1073/pnas.1012344107
Plasmid: CERV2 RBD-IgG1 Fc expression vector	This paper	N/A
Plasmid: LNCX	Lopez-Sanchez, JBC, 2020[70]	https://doi.org/10.1074/jbc.RA119.011376
Plasmid: LNCX FLAG human CTR1	This paper	N/A
Plasmid: LNCX FLAG cat CTR1	This paper	N/A

(*Continued on next page*)

Continued

REAGENT or RESOURCE	SOURCE	IDENTIFIER
Software and algorithms		
GraphPad Prism	N/A	https://www.graphpad.com/scientific-software/prism/
FlowJo™ v10	N/A	https://www.bdbiosciences.com/en-us/products/software/flowjo-v10-software

RESOURCE AVAILABILITY

Lead contact

Further information and requests for resources and reagents should be directed to and will be fulfilled by the lead contact, Jean-Luc Battini, jean-luc.battini@irim.cnrs.fr.

Materials availability

Plasmids generated in this study are available without restrictions upon request to the lead contact.

Data and code availability

- All original data not included in the manuscript will be shared by the lead author upon request.
- This paper does not report original code.
- Any additional information required to reanalyze the data reported in this paper is available from the lead contact upon request.

EXPERIMENTAL MODEL AND STUDY PARTICIPANT DETAILS

Cell lines

HEK (Human Embryonic Kidney) 293T, hamster CHO (Chinese Hamster Ovary), and cat FEA (Feline embryonic fibroblast)[66] and CRFK (Crandell feline kidney, kind gift from A. Cimarelli) cell lines were maintained in DMEM (Dulbecco's Modified Eagle's Medium, Gibco) supplemented with 10% fetal bovine serum (FBS, Sigma), 1% antibiotics (penicillin-streptomycin) and non-essential amino acids (Gibco). Cells were cultivated under humid atmosphere in a 5% CO_2 incubator at 37°C. *CTR1* KO 293T cells were generated previously.[34]

Primary cells

Peripheral blood mononuclear cells (PBMCs) were isolated from whole blood of male domestic cats (1 mL taken in EDTA tubes) obtained at veterinary clinics with the consent of the cat owners.

METHOD DETAILS

Plasmids

Human and feline CTR1 cDNA were tagged either at the C-terminal end with 3 copies of the HA tag from the pCHIX vector[24] or at the N-terminal part with the 3 copies of the FLAG tag from the 3XFLAG-pCMV-10 vector (Sigma), and introduced in the pLXSN and pLNCX[38] retroviral vectors respectively. The Refrex1 ligands were derived from *ERV-DC7* and *ERV-DC16 env* genes and introduced in the pCHIX vector. The resulting ligands harbored 3 copies of the HA tag in place of the stop codon. The DC16 Refrex1 ligand was also fused to the mouse IgG1 Fc domain as for all the RBD ligands used in this study. Chimpanzee endogenous retrovirus type 2 (CERV2) RBD ligand (first 215 residues) was derived from a consensus CERV2 *env* expression vector ([37], kind gift of Paul Bieniasz) and fused to mouse IgG1 Fc domain.

Viral productions and infections

pLXSN or pLNCX vectors pseudotyped with the vesicular stomatitis virus G protein (VSV-G) were produced by cotransfecting 293T cells with the LXSN vectors carrying the human and feline CTR1 cDNAs,[34] the MLV Gag-Pol expression vector pC57GPBEB[67] and the VSV-G Env expression vector pCSIG.[68] Viral supernatants were harvested 48 hours after transfection, filtered through 0.45 μm pore-size filters and used to transduce CHO cells followed by G418 selection one day later. CSGW lentiviral vectors expressing the enhanced green fluorescent protein (EGFP) were produced by cotransfecting 293T cells with the pCSGW[69] lentiviral vector, the HIV1 psPAX2 *gag-pol* expression vector, and the Env expression vectors from VSV, ERV-DC14 or FeLV-C. They were used to infect for 48 hours $1x10^4$ cells/well seeded the day before in 96-well plate. Cells were then resuspended in 50 μl trypsin and 100 μl PBA (PBS with 2% FBS) and analyzed on a Novocyte flow cytometer (Acea, Biosciences, Inc). Data analyses measuring the percentage of EGFP-positive infected cells were performed using FlowJo software.

Monitoring cell surface expression of retroviral receptors/solute carriers using retroviral RBD ligands

Detection of CTR1, FLVCR1, GLUT1 and SLC20A2 at the plasma membrane was performed using soluble receptor-binding domains (RBD) Env derived from: ERV-DC14 (first 278 residues),[34] ERV-DC16/refrex1 (first 297 residues) and CERV2 (first 215 residues) for CTR1; FeLV-C (first 235 residues) for FLVCR1; HTLV2 (first 184 residues) for GLUT1; and Amphotropic-MLV retrovirus (first 448 residues) for SLC20A2 fused to a mouse IgG1 Fc domain.[24] The Refrex1 DC16 ligand was also fused to 3 copies of the HA tag at the its C-terminus. RBD ligands were produced and used as previously described.[70] Human CTR1 was also detected using a mouse anti-CTR1 monoclonal antibody (Proteintech). FLAG-tagged human and cat CTR1 were detected using the anti-FLAG M2 mouse monoclonal antibody (Sigma). Briefly, $1x10^5$ cells were detached with trypsin 0.5%+1mM EDTA for FEA and CRFK cells and mechanically for 293T cells, resuspended in 100 μl PBA containing the different RBDs and incubated at 37°C for 30 min. Cells were then washed twice with cold PBA and labeled for 20 min on ice with Alexa 488- or Alexa 647-conjugated anti-mouse IgG1 antibodies (1:400). For the Refrex1/DC16HA ligand, cells were labeled 30 minutes at 4°C with an anti-HA antibody diluted at 1:200 in PBA. For the mouse anti-CTR1 and mouse anti-FLAG M2 antibodies, a 30-minute incubation at 4°C was performed at a 1:400 and 1:300 dilution respectively before the secondary antibody staining. Cells were then washed in PBA and analyzed on a Novocyte flow cytometer (Acea, Biosciences, Inc). Data analysis was performed using FlowJo software version 10. When indicated, 293T cells were incubated in FEA or CRFK cells conditioned medium, or incubated overnight with 100 μM $CuCl_2$ or $MgCl_2$.

RNA isolation, synthesis of cDNA, RT-PCR and RT-qPCR

Total RNA ($5x10^6$ cells) was extracted from FEA, CRFK cell lines or cat PBMCs by using the RNeasy Plus Mini Kit. RNA from FEA, CRFK cells or cat PBMCs were primed with Oligo(dT)18 and cDNA were synthetized using the Superscript II First Strand Synthesis System. A 523bp fragment of ERV-DC7 or ERV-DC16 env genes was then amplified by PCR using One Taq DNA Polymerase with the following primers: DC7/16-Fwd and DC7/16-Rev (key resource table). The PCR products were agarose gel purified using the PCR clean-up Gel Extraction kit according to manufacturer's protocol and used for direct Sanger sequencing. For RT-qPCR, cells were lysed and RNA extracted using the Luna Cell Ready Lysis Module according to the manufacturer's protocol. RT-qPCR on extracted RNA was performed using the Luna One-Step RT-qPCR Kit. The samples were analyzed using a LightCycler 480 instrument (Roche) or a CFX Opus 384 Real-Time PCR system (Biorad). qPCR primers for ERV-DC *env* genotypes I, II, III have been previously described.[51] They can be found, along with qPCR for feline genes, in key resource table.

Immunoblotting

Cells were lysed in 50 mM Tris-HCl (pH 8.0), 100 mM NaCl, 1 mM $MgCl_2$, 1% Triton X-100, and protease inhibitors. Cell extracts were separated on a 12.5 % SDS acrylamide gel, transferred to PVDF membranes and protein expression was detected using anti HA (1:5000) followed by horseradish peroxidase (HRP)-conjugated anti-rat antibodies (1:10000), or anti CTR1 monoclonal antibody (1:1000) or anti FLAG M2 monoclonal antibody followed by HRP-conjugated anti-mouse antibodies (1:10000), or anti CCS polyclonal antibody followed by HRP-conjugated anti rabbit antibodies (1:2000) or HRP-conjugated anti-ß-actin (1:100000) antibodies. Signals were visualized using the Luminata Forte detection reagent and recorded using the Chemidoc gel imaging system (Biorad).

Crystal violet viability staining

FEA and CRFK cells were seeded in 24-well plates at a density of $1x10^5$ and $8x10^4$ cells per well respectively. The next day, they were transfected with siDC7/16 or siLuc as a control using JetPrime according to the manufacturer's protocol. 6h later, the medium was changed to medium without BCS or containing increasing concentrations of the copper chelator Bathocuproine disulfonic acid (BCS)(100 μM, 200 μM). 3 days post-siRNA transfection, pictures of each well were taken using a Nikon Eclipse Ts2 microscope. Cells were then washed with PBS and fixed with formalin for 20min at room temperature. Formalin was removed before adding Crystal violet 0.5% in 20% methanol and incubating a minimum of 1h at room temperature. Crystal violet was then washed 3 to 4 times in water before being left to dry. Once dry, the plate was scanned to get an image of the overall density of cells in all wells. Crystal violet was then solubilized in 1 mL 80% methanol and 100 μL of solution were distributed in 3 replicate wells of a 96-well plate. Absorbance at 570 nm was read using a Infinite F200PRO microplate reader (Tecan).

Copper dosage

FEA, CRFK and 293T cells were seeded in 6-well plates at a density of $5x10^5$ per well. The next day, they were transfected using JetPrime according to the manufacturer's protocol with siDC16 or siLuc as a control for FEA and CRFK or with DC7, DC16, DC7+16 or pCHIX as a control for 293T cells. The medium was changed 4h later and replace by a medium with 100 μM BCS. The next day, the medium was removed and cells were incubated 1h with 25 μM $CuCl_2$. Then, they were washed twice with cold PBS and 200 μl Pierce™ IP lysis buffer supplemented with protease inhibitors was added in each well. A portion (5 μl) was kept to quantify the total amount of proteins using Pierce™ BCA protein assay kit. 5 ml of HNO3 5% were added to each sample and they were placed 1h at 95°C. Copper and magnesium dosage were then quantified using the inductively coupled plasma mass spectrometry (ICP-MS) method at the OSU OREME platform of Montpellier University.

Viability assay

FEA and CRFK cells were seeded in 6-well plates at a density of $3x10^5$ cells per well. The next day, they were transfected with with 100 pmol of siDC7/16, DC16 or siLuc or siGPX4 as controls using JetPrime according to the manufacturer's protocol. For rescue experiments 50 pmol of siRNA along with 1 μg of plasmid DNA were cotransfected. 6h later, cells were harvested using trypsin 0.5% + 1 mM EDTA and then distributed into 6 technical replicates in a 96-well plate. Cell viability was measured 48h later (or otherwise indicated) using CellTiter 96® AQueous One Solution Cell Proliferation Assay according to the manufacturer's instructions. Absorbance was measured at 490 nm using an Infinite F200PRO microplate reader (Tecan).

ATP measurement

FEA and CRFK cells were seeded in 96-well plates at a density of $3x10^4$ cells per well. The next day, they were transfected with siDC7/16, siDC16 or siLuc or siGPX4 as controls using JetPrime according to the manufacturer's protocol. ATP measurement was performed using the ATPlite Luminescence Assay System according to the manufacturer's protocol.

Annexin V/propidium iodide staining

FEA and CRFK cells were seeded in 6-well plates at a density of $3x10^5$ and $2.5x10^5$ cells per well respectively. The next day, they were transfected with siDC7/16, siDC16 or siLuc as a control using JetPrime according to the manufacturer's protocol. The medium was changed 6h later. 24h post-siRNA transfection, cells were washed with PBS and detached using Trypsin 0.5%+1mM EDTA for 5 min at 37°C. Cells were collected using complete medium and distributed into 3 technical replicates in a 96-well plate. Cells were then washed with PBS and stained for Annexin V and propidium iodide (PI) using the eBioscience Annexin V-FITC Apoptosis detection kit according to manufacturer's instructions with slight modifications. Briefly, cells were washed once in 1X binding buffer then Annexin V was diluted 1:40 in binding buffer and 40 μL was added per well. Cells were resuspended and incubated for 15 min at room temperature in the dark. After one wash in binding buffer, cells were resuspended in 150 μL of binding buffer containing PI diluted 1:20 and directly analyzed using a Novocyte flow cytometer (Acea, Biosciences, Inc). Data analysis was performed using FlowJo software. One well was not stained with Annexin V and stained with PI only to be used as a gating control.

ROS staining

Cells were transfected with siRNA, incubated and collected as described above. Cells were then distributed into 3 technical replicates in a round-bottom 96-well plate and washed twice with PBS. Cells were resuspended in 50 μL of PBS containing 2 μM of DCFDA and incubated at 37°C in the incubator for 30 min to allow for dye loading. After 1 wash in PBS, cells were resuspended in 50 μL PBS+SYTOX Red diluted 1:1000 and incubated for 15 min at room temperature in the dark. 100 μL of PBS was then added per well and cells resuspended before analysis using a Novocyte flow cytometer (Acea, Biosciences, Inc). Data analysis was performed using FlowJo software. One well was not stained with DCFDA to be used as a control of background cell fluorescence.

PBMCs purification

Peripheral blood mononuclear cells (PBMCs) were isolated from whole blood of cats using Ficoll (Histopaque). Briefly, total sample of whole blood of each cat was deposited on 2mL of the density gradient and centrifuge at 600g during 30min at room temperature without brake. The ring of PBMCs was carefully recovered and wash twice in PBS. The cells were then resuspended in RPMI (Roswell Park Memorial Institute)-1640 medium supplemented with 10% fetal bovine serum (FBS, Sigma), 1% antibiotics (penicillin-streptomycin) and when indicated, were incubated overnight with 250 μM $CuCl_2$.

QUANTIFICATION AND STATISTICAL ANALYSIS

Statistical analyses were performed using GraphPad Prism 6 software. The data were expressed as the mean ± SEM. Statistical tests and number of independent experiments are indicated in the figure legends.The results were considered statistically significant at a p-value <0.05 (*), <0.01 (**), <0.001 (***) or <0.0001 (****).

Cell Reports, Volume *42*

Supplemental information

A co-opted endogenous retroviral envelope promotes cell survival by controlling CTR1-mediated copper transport and homeostasis

Sandrine Tury, Lise Chauveau, Arnaud Lecante, Valérie Courgnaud, and Jean-Luc Battini

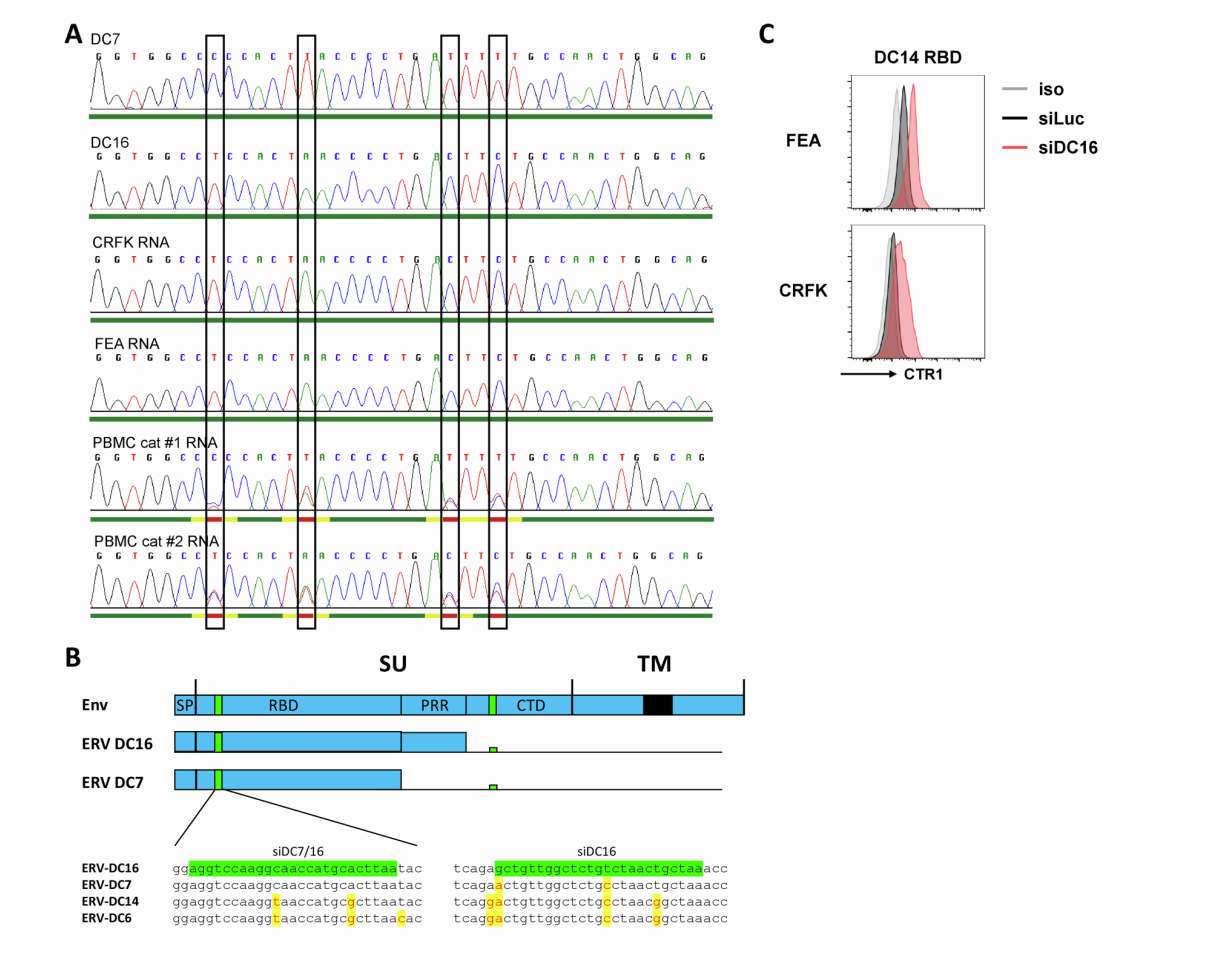

Figure S1: ERV-DC7/ERV-DC16 sequences and siRNA targeting

(A) Direct DNA Sanger sequencing chromatograms showing sequence polymorphisms of a fragment of Refrex1 (DC7 or DC16) in cDNA from FEA, CRFK cells or cat PBMCs**.** Total RNAs were extracted from the indicated cells and sanger sequencing was performed on RT-PCR amplified cDNA. A 39-bp DNA fragment starting at position 178 from start codon and containing 4 differences between ERV-DC7 and ERV-DC16 env is shown.

(B) Schematic representation of ERV-DC7 and ERV-DC-16 Env organization. Both Env contain a signal peptide (SP) and a receptor-binding domain (RBD). Only DC16 contains an extra proline-rich region (PRR). SU: surface unit; TM: transmembrane unit; CTD: C-terminal domain. Partial sequence alignments surrounding the siDC7/16 and siDC16 sequences (highlighted in green) are shown. ERV-DC7 and 16 are prototypes of genotype group II, ERV-DC14 of genotype group I and ERV-DC6 of genotype group III.

(C) Silencing of DC16 increases DC14-RBD binding in FEA and CRFK cells. Binding was performed 37°C for 30 minutes following by incubation with an Alexa 647-conjugated secondary anti mouse IgG1 antibody (1:400) at 4°C for 20 minutes before flow cytometry acquisition.

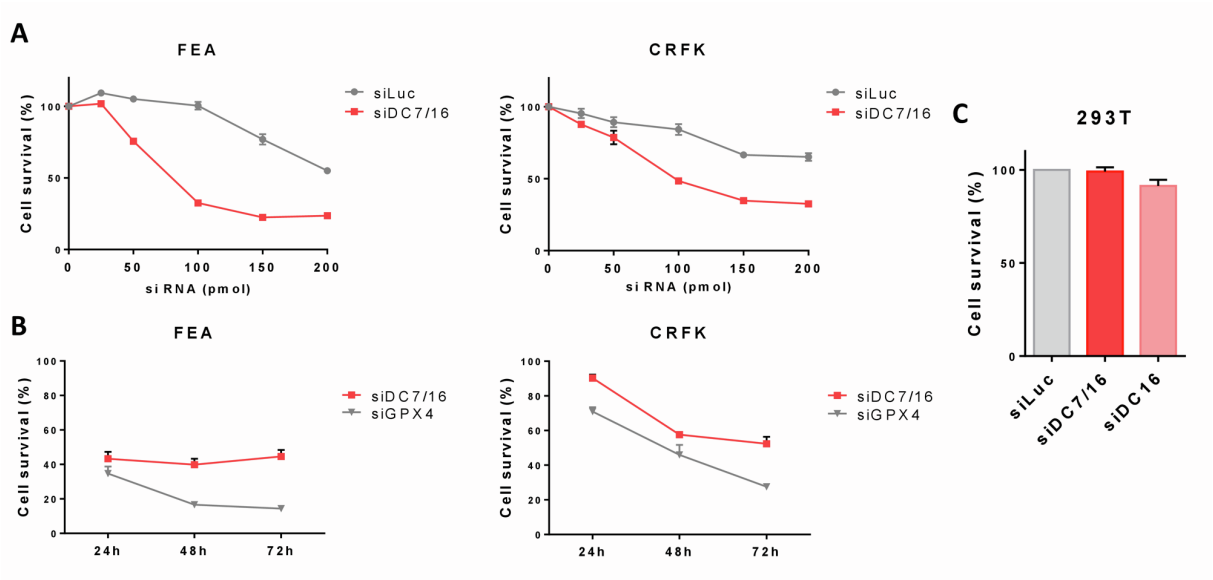

Figure S2: FEA, CRFK and 293T cell toxicity following siDC7/16 transfection

A) Cell toxicity is dose-dependent. Feline FEA and CRFK cells transfected with increasing quantities (25-200 pmol) of siDC7/16 or siLuc were evaluated for cellular viability 48h post transfection using CellTiter 96® AQueous One Solution Cell Proliferation Assay.

(B) Cell toxicity is time-dependent. Feline FEA and CRFK transfected with a siDC7/16 or siLuc control were evaluated for cellular viability 24h, 48h or 72h post transfection using CellTiter 96® AQueous One Solution Cell Proliferation Assay.

(C) Human 293T cells are not sensitive to siDC7/16 and siDC16 transfection. Human 293T cells transfected either with siLuc, siDC7/16 or siDC16 were evaluated for cellular viability 48h post transfection using CellTiter 96® AQueous One Solution Cell Proliferation Assay

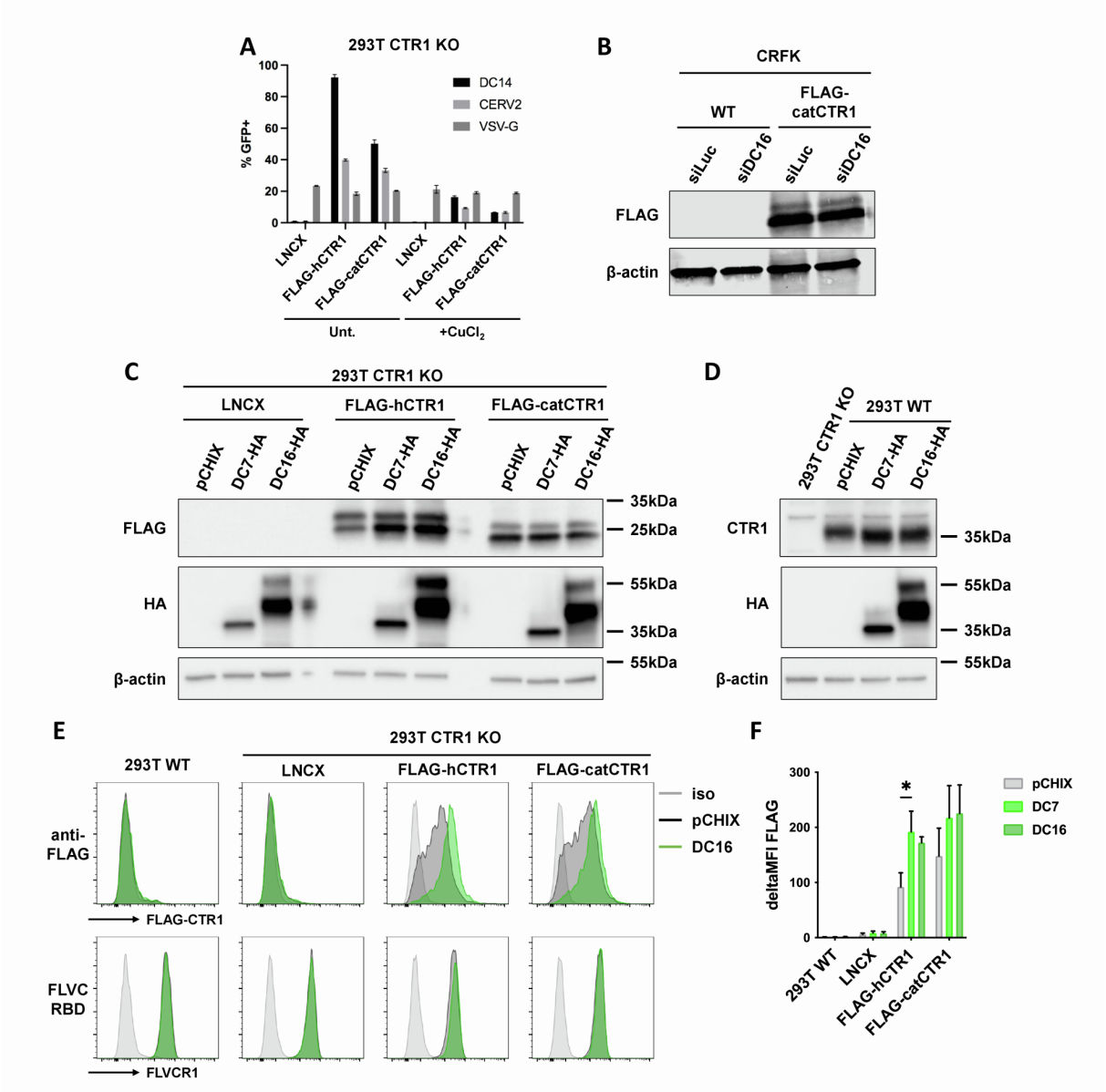

Figure S3: Refrex1 regulation of CTR1 activity does not involve degradation or downregulation of cell surface expression.

(A) human (h) and feline (cat) FLAG-CTR1 are functional retroviral receptor for GFP MLV vector pseudotyped with DC14 or CERV2 Env.

(B) siDC16 does not affect protein levels of feline FLAG-CTR1 expressed in CRFK cells transfected with siLuc or siDC16

(C) Overexpression of DC7 or DC16 does not affect protein levels of FLAG-hCTR1 or catCTR1 expressed in 293T CTR1 KO cells transfected with the pCHIX empty vector or DC7-HA or DC16-HA Env vectors.

(D) Overexpression of DC7 or DC16 does not affect protein levels of endogenous human CTR1 in 239T WT cells transfected with the pCHIX empty vector or DC7-HA or DC16-HA Env vectors.

(E) Overexpression of DC16 does not affect cell surface expression of FLAG-hCTR1 or catCTR1 expressed in 293T CTR1 KO cells transfected with the pCHIX empty vector or DC16-HA Env vectors as assessed by flow cytometry using an anti-FLAG antibody

(F) Comparison of delta mean fluorescence intensity of anti-FLAG M2 antibody compared with non-specific mock staining (grey histogram) obtained from (E) (n=3). Data are mean ± SEM from n=3 experiments. Two-way ANOVA with Dunnett's multiple comparisons test * = $p \leq 0.05$.

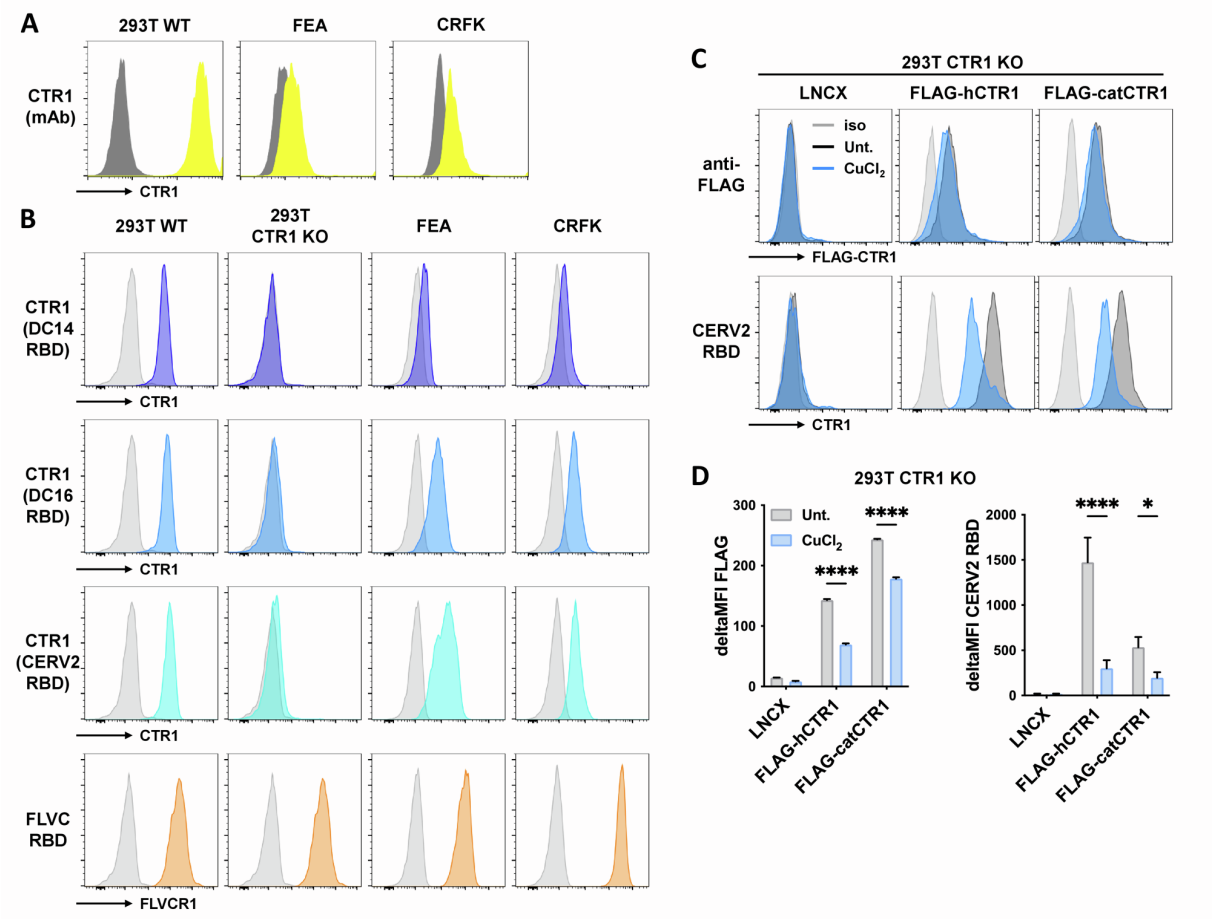

Figure S4: Detection of CTR1 at the surface of feline cells by DC14, DC16 and CERV2 RBD and CTR1 antibody

(A) 293T and feline FEA and CRFK cells were evaluated for CTR1 cell surface expression by flow cytometry using an anti-CTR1 antibody.

(B) 293T, 293T CTR1 KO, FEA and CRFK cells were evaluated for CTR1 cell surface expression by flow cytometry using RBD ligands from ERV-DC14, DC16 and CERV2 Env. FLVC RBD was used as a control.

(C) Detection of human and cat FLAG-CTR1 at the cell surface of transduced 293T CTR1 KO cells by flow cytometry using an anti-FLAG antibody after an overnight treatment with 100 µM $CuCl_2$ (Unt.=untreated).

(D) Comparison of delta mean fluorescence intensity of anti-FLAG M2 antibody compared with non-specific mock staining (grey histogram) obtained from (C). Data are mean ± SEM from n=3 experiments. Two-way ANOVA with Sidak's multiple comparisons test * = $p \leq 0.05$; **** = $p \leq 0.0001$.

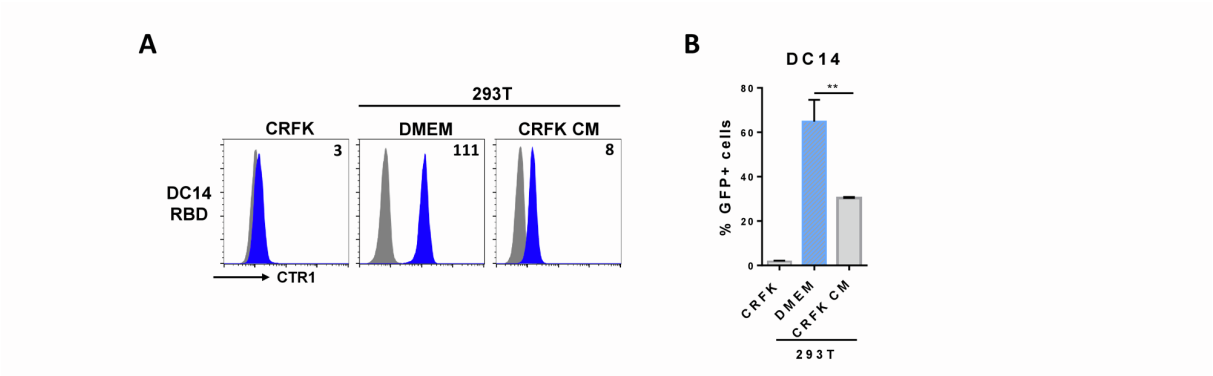

Figure S5: Refrex1/DC16 is present in CRFK CM

(A) Detection of DC14RBD binding was performed on CRFK cells as well as on 293T cells pre-incubated for 5 hours with either DMEM or CM from CRFK cells by flow cytometry. Numbers indicate the specific change in mean fluorescence intensity compared with non-specific mock staining (grey histogram of a representative experiment (n=3).

(B) Cells treated as in A were evaluated for their sensitivity to infection by EGFP lentiviral vector pseudotyped with ERV-DC14 Env. Data are means ± SEM from n=3 experiments. Student unpaired t-test, **=p≤0.01.

Table S1

REAGENT or RESOURCE	SOURCE	IDENTIFIER
Oligonucleotides		
siRNA targeting Luc: siLuc 5'-CUUACGCUGAGUACUUCGA -3'	Giovaninni et al, 2013	http://dx.doi.org/10.1016/j.celrep.2013.05.035
siRNA targeting ERV-DC7/16: siDC7/16 5'-AGGTCCAAGGCAACCATGCACTTAA-3'	This paper	N/A
siRNA targeting ERV-DC16: siDC16 5'-GCTGTTGGCTCTGTCTAACTGCTAA-3'	This paper	N/A
siRNA targeting feline GPX4: siGPX4 5'- AGGACATCGATGGACACATGGTTAA -3'	This paper	N/A
DC7/16, Fwd 5'-AATTGGAGCTAAAAATGTCGGG-3'	This paper	N/A
DC7/16, Rev 5'-TTCCCAATAATGATACCCTTC-3'	This paper	N/A
Genotype I, Fwd 5'-GCTTGCACTTCCACCAGTTG-3'	Kuse et al, J Virol, 2016	https://doi.org/10.1128/jvi.00716-16
Genotype I, Rev 5'-ACCTGTTCCTGTCTTGCGTAG-3'	Kuse et al, J Virol, 2016	https://doi.org/10.1128/jvi.00716-16
Genotype II, Fwd 5'-ACCTGTTCCTGTCTTGCGTAG-3'	Kuse et al, J Virol, 2016	https://doi.org/10.1128/jvi.00716-16
Genotype II, Rev 5'-TGCCAACTGGTTTTGTTACTTATG-3'	Kuse et al, J Virol, 2016	https://doi.org/10.1128/jvi.00716-16
Genotype III, Fwd 5'-GCCTCCCTACCCGACTTCC-3'	Kuse et al, J Virol, 2016	https://doi.org/10.1128/jvi.00716-16
Genotype III, Rev 5'-AGGGGGTTTAGCCGTTAGG-3'	Kuse et al, J Virol, 2016	https://doi.org/10.1128/jvi.00716-16
Atp7a, Fwd 5'-GCTGTGTGGCTTGATTGCTA-3'	This paper	N/A
Atp7a, Rev 5'-TTTCCCCTCCTCCTGAAGTT-3'	This paper	N/A
Atp7b, Fwd 5'-CTGTAAAGAGGAGCTGGGAAC-3'	This paper	N/A
Atp7b, Rev 5'-CCTCCACGTTGCTGACTTTA-3'	This paper	N/A
Commd1, Fwd 5'-CATGTGACCAAGCTGCTGTT-3'	This paper	N/A
Commd1, Rev 5'-CAGGCAACCCTGACTTGTTT-3'	This paper	N/A
Ctr1, Fwd 5'- GGAACCATCCTTATGGAGACAC-3'	This paper	N/A
Ctr1, Rev 5'-GCTGATGACCACTTGGATGATA -3'	This paper	N/A
Mt1/2, Fwd 5'CCTGCAAGAAGAGCTGCTG-3'	This paper	N/A
Mt1/2, Rev 5' CAGCTGCACTTGTCCGATG-3'	This paper	N/A
Gapdh, Fwd 5'-GTCTTCCTGCGACTTTAACAGTG-3'	This paper	N/A
Gapdh, Rev 5'-ACCACCCGGTTGCTGTAGCCAA-3'	This paper	N/A